https://doi.org/10.5194/egusphere-2026-365
Preprint. Discussion started: 6 February 2026

Human-Centred Design approaches to Tsunami Mitigation under Sea Level Rise in Kesennuma, Japan.

Hayley Leggett[1], Muhammad Daffa Al Farizi[2], Muhammad Rizki Purnama[1], Anawat Suppasri[2], Fumihiko Imamura[2]

[1]Department of Civil and Environmental Engineering, Graduate School of Engineering, Tohoku University, 6-6-06 Aramaki Aza, Aoba, Sendai, Miyagi, 980-8579, Japan
[2]International Research Institute of Disaster Science, Tohoku University, 468-1 Aoba, Aramaki, Aoba-ku, Sendai, Miyagi, 980-8572, Japan

Correspondence to: Hayley Leggett (hayley.leggett.p8@dc.tohoku.ac.jp)

Abstract. Human-centred design (HCD) is increasingly prioritised as studies show human experience is critical in infrastructure use, and recent policies call for more socially responsive design. Tsunami impacts intensify as sea level rise (SLR) raises baseline water levels and reduces existing defence effectiveness, yet HCD informed approaches are rarely tested under projected SLR. Based on identified infrastructure preferences in Kesennuma City, Japan, we develop three multi-layered defence configurations: an environmentally integrated eco hybrid system (Design 1), a discreet open feeling barrier system (Design 2), and a reinforced high-performance system (Design 3). Using TUNAMI-N2 numerical modelling, 150 simulations combine three tsunami sources, five SLR conditions, and five defence states. Results for inundation extent, fatality rates, and economic loss show a consistent hierarchy: Design 3 achieves the strongest containment, while Design 2, which more closely aligns with residents' preferences for openness and access, delivers near equivalent reductions typically within 10–15 percent. Design 1 provides only limited hazard reduction and is unsuitable as a standalone mitigation system. We show that HCD informed configurations can deliver strong technical performance and support a shift toward socially integrated, multi-layered tsunami protection under rising sea levels.

1 Introduction

The interaction between tsunami and sea level rise (SLR) has become a central consideration in coastal hazard mitigation and infrastructure design. Tsunami generated by megathrust earthquakes along subduction zones displace vast volumes of seawater and can devastate coastlines within minutes (Fuji et al., 2024; Lay et al., 2005; Satake, 2015). Long-term SLR amplifies tsunami impacts by raising baseline sea levels, increasing overtopping, and reducing the effectiveness of coastal defences (Koyano et al., 2022; Chua et al., 2024). Together, these processes create compound hazards that allow tsunami waves to travel further inland and increase inundation extent and damage potential (Grezio et al., 2017; Welsh, 2023). Traditional disaster risk reduction (DRR) strategies dominated by hard-engineered structures such as seawalls and breakwaters have shown limited adaptability to changing environmental baselines. Recent approaches promote multi-layered

https://doi.org/10.5194/egusphere-2026-365
Preprint. Discussion started: 6 February 2026

protection systems that integrate physical, ecological, and social measures (UNDRR, 2022; Takabatake et al., 2020). Within this context, Human Centred Design (HCD) offers a framework for rethinking how tsunami mitigation infrastructure can balance engineering performance with the lived experiences and values of coastal communities (Giacomin, 2014; Charlesworth & Fien, 2022). HCD emphasises empathy, participation, and iteration to ensure infrastructure is functional, trusted, and suited to local contexts. In DRR, it reframes defences as socio-technical systems where perception and everyday interaction influence safety outcomes (Bell et al., 2022; Wolff, 2021). By embedding community perspectives in design, HCD enables infrastructure that is both technically robust and socially meaningful. This approach is especially relevant in Japan, where post-2011 reconstruction raised debate over how large-scale mitigation can coexist with the social and aesthetic character of coastal settlements (Strusińska-Correia, 2017; Aoki, 2018).

This relationship between community perception and infrastructure performance was explored in Kesennuma, Japan, through empirical work by Leggett et al. (2025). Using mixed methods combining surveys, interviews, and observation, the study examined how residents perceive and engage with tsunami infrastructure and DRR practices. Residents valued visibility and connection to the sea, integration of defences with the landscape, and the use of alternative materials to concrete. Trust in infrastructure depended on both perceived safety and how well designs reflected local identity. While not framed within HCD, these results highlight the importance of incorporating user experience and local values into mitigation planning. However, the study did not evaluate whether such community-informed designs can maintain technical performance under future conditions, including SLR. Kesennuma's context provides an opportunity to address this gap. Located on the Sanriku Coast of Miyagi Prefecture, the city's ria coastline, dependence on fisheries, and low-lying settlement make it highly vulnerable to tsunami and SLR (Otsuyama & Shaw, 2021). Following the 2011 Great East Japan Earthquake and Tsunami (GEJE), Kesennuma incorporated elements of participatory reconstruction, engaging residents and local authorities in selected decisions on seawall design and the use of adaptive barriers (Ueda & Shaw, 2014). Following this, features such as glass windows and hydraulic flap gates were installed and preserved sightlines while maintaining protection (Tashiro & Sakisaka, 2015). This experience reflects the human centred ethos that informs the present study, which applies community-derived design principles to explore how socially informed infrastructure could perform under future climatic scenarios.

The objectives of this study are threefold: (1) to develop multi-layered tsunami defence systems that integrate HCD principles identified through community research in Kesennuma; (2) to evaluate their performance under combined tsunami and SLR scenarios using numerical modelling; and (3) to assess whether community-informed, human centred infrastructure can balance social integration with engineering effectiveness to strengthen long-term coastal resilience. Through this approach, the study links social understanding with quantitative performance assessment, advancing both theoretical and applied dimensions of human centred DRR.

https://doi.org/10.5194/egusphere-2026-365
Preprint. Discussion started: 6 February 2026

2 Background

2.1 Tsunami exposure and multi-layered mitigation in Kesennuma

Kesennuma, located on the Sanriku Coast of Miyagi Prefecture, faces the Pacific Ocean near the Japan Trench, one of the world's most active subduction zones. The city's ria coastline amplifies tsunami wave energy as it funnels through narrow inlets, producing higher run-up and inundation than on open coasts (Otsuyama & Shaw, 2021). Historical records show repeated large-scale tsunami, including the 1896 Meiji Sanriku and 1933 Showa Sanriku events, both of which caused severe casualties and extensive destruction across the Sanriku region (Shibayama et al., 2013). The GEJE was the most catastrophic, producing local run-up heights exceeding 20 metres, inundating central Kesennuma, and destroying large portions of the fishing port, coastal industry, and housing. More than 1,300 people were killed and over 15,000 buildings were damaged or destroyed (Otsuyama & Shaw, 2021). The GEJE exposed the limitations of Japan's pre-2011 tsunami countermeasures, which had been designed primarily on the basis of historical tsunami heights, particularly those recorded during the 1960 Chile tsunami (Hatamura & Iino, 2014; Koshimura & Shuto, 2015; Strusińska-Correia, 2017). Many seawalls were overtopped or collapsed, revealing weaknesses in foundation design, construction methods, and the assumption that past events represented the upper bound of hazard potential.

After the GEJE, the MLIT introduced a national framework promoting multi-layered tsunami countermeasures that integrated structural and non-structural approaches (Strusińska-Correia, 2017; Takabatake et al., 2020). Level 1 (L1) tsunamis represent relatively frequent events with return periods of up to around 100 years and are used as the design basis for standard coastal protection infrastructure. Level 2 (L2) tsunamis correspond to rare, large-magnitude events with recurrence intervals of up to roughly 1000 years, reflecting extreme, low-probability scenarios such as the 2011 GEJE. Primary structures such as seawalls and breakwaters were intended to reduce inundation and provide time for evacuation during L1 events, while secondary measures, including embankments, roads, and green infrastructure, slowed flow velocity and reduced damage during L2 events (Fig. 1). Non-structural strategies such as hazard zoning, evacuation planning, and education complemented these physical layers. These principles were further institutionalised through the Technical Standards for Coastal Facilities (MLIT, 2013a) and the National Resilience Plan (MLIT, 2015), which provide national guidance on integrated coastal defence and adaptive risk management. In Kesennuma, reconstruction was shaped by local priorities, physical constraints, and the preferences of residents rather than by national design logic. The city's approach emphasised maintaining visibility, accessibility, and cultural continuity along the coast while improving safety through structural reinforcement and land-use modification. Its topography, economic dependence on fisheries, and strong civic culture required solutions that balanced protection with the preservation of community identity and daily life.

https://doi.org/10.5194/egusphere-2026-365
Preprint. Discussion started: 6 February 2026

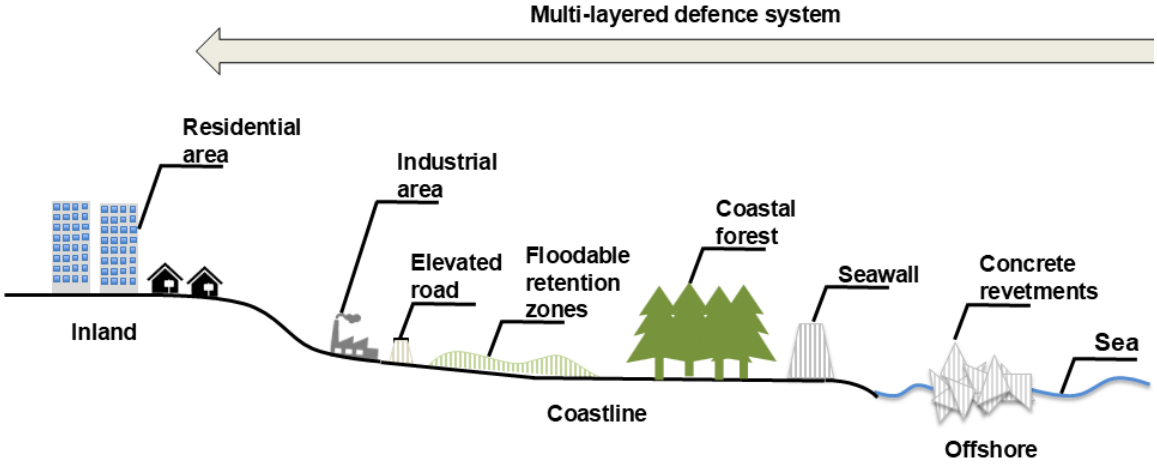

Fig. 1: Example of a multi-layered defence system promoted by the MLIT post-2011.

2.2 Post-GEJE reconstruction and existing tsunami defences

Reconstruction in Kesennuma involved the redevelopment of coastal infrastructure through a combination of large concrete seawalls, raised roads, hydraulic barriers, and embankments designed to withstand tsunami seen in Fig. 2. These projects were funded and overseen jointly by national and prefectural agencies but implemented through local consultation processes led by the Kesennuma City Office. Major reconstruction works were completed by 2019 under the national Reconstruction Agency programme, allowing sufficient time for assessment of performance and public reception. Unlike many neighbouring municipalities, Kesennuma invited public participation in reconstruction planning, allowing residents to express concerns about the visual and spatial effects of new seawalls and the potential loss of connection to the sea (Ueda & Shaw, 2014). Participation focused primarily on negotiating visibility, access, and aesthetic impact rather than redefining engineering specifications. Residents' input led to adjustments such as lowering seawall heights in certain areas, incorporating reinforced glass windows into the seawall along the port, and adopting hydraulically operated barriers to preserve sightlines and maintain the usability of waterfront areas (Tashiro & Sakisaka, 2015).

These locally driven changes sought to balance safety with cultural and experiential dimensions of the coastal landscape. However, not all responses were positive. Some regional media and neighbouring municipalities criticised Kesennuma's participatory stance as overly individualistic or "selfish," arguing that its negotiations slowed reconstruction or potentially compromised safety standards. This criticism reflected deeper national tensions between locally driven adaptation and Japan's highly centralised, technocratic reconstruction model (Ueda & Shaw, 2014). The resulting defence system represents a hybrid between national engineering requirements and locally negotiated modifications. Primary concrete seawalls act as

https://doi.org/10.5194/egusphere-2026-365
Preprint. Discussion started: 6 February 2026

the first line of protection, while secondary structures such as adaptive embankments, elevated roads, and hydraulic flap gates provide additional layers of defence. Complementary measures, including evacuation buildings, hazard mapping, and regular community drills coordinated by the city's Crisis Management Division, strengthen non-structural preparedness. Together, these measures demonstrate Kesennuma's effort to achieve physical safety while retaining visibility, accessibility, and continuity with the coastal environment.

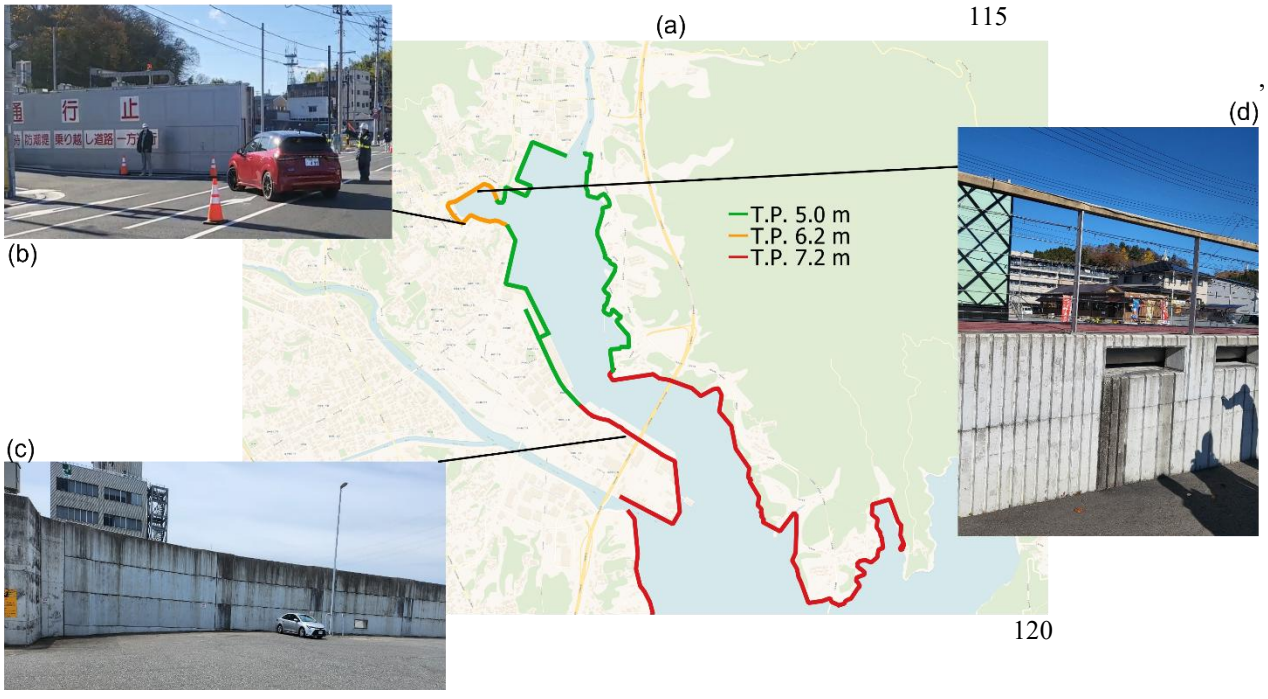

Fig. 2: Current tsunami mitigation infrastructure in Central Kesennuma (a) Seawall heights (b) Automatic seagate controlled remotely by J Alert in Tokyo (c) Tallest concrete seawall observed at Kesennuma Port (d) Barrier hydraulically activated by water ingress, increasing barrier height by 1 metre. Base map from OpenStreetMap contributors.

2.3 Integrating community perspectives and future conditions

Kesennuma's post-GEJE reconstruction provides a critical foundation for examining how HCD principles can inform tsunami mitigation infrastructure. While earlier research in the city (Leggett et al., 2025) explored residents' attitudes toward infrastructure, hazard awareness, and personal DRR plans, it was not explicitly framed through an HCD lens. Nevertheless, its results align closely with HCD principles, highlighting that trust in protective structures depends on how well they reflect local identity, integrate with daily life, and maintain visible and physical connections to the sea. Residents expressed support for measures that contribute positively to the urban landscape, emphasising multifunctionality and social integration alongside safety. These insights underline that effective tsunami mitigation requires more than structural robustness; it also depends on whether infrastructure supports social and psychological dimensions of resilience.

A key gap, however, remains in assessing whether infrastructure reflecting community preferences can maintain technical performance under projected SLR. As baseline water levels rise, the frequency and depth of overtopping are expected to

https://doi.org/10.5194/egusphere-2026-365
Preprint. Discussion started: 6 February 2026

increase, while reduced bottom friction and altered flow dynamics may compromise structural integrity and the functional life of defences (Koyano et al., 2022; Chua et al., 2024). Addressing this interaction between community-driven design and physical performance is critical for developing future-ready tsunami infrastructure. Building on Kesennuma's distinct reconstruction context, this study evaluates the technical performance of alternative multi-layered defence configurations that integrate community-derived principles through numerical simulation of combined tsunami and SLR scenarios. By uniting HCD-informed design logic with quantitative modelling, the study aims to determine whether infrastructure that aligns with local social priorities can also deliver long-term engineering resilience. The following section outlines the methodology used to develop and test these configurations.

3 Data and Methodology

The performance of multi-layered tsunami mitigation designs in Kesennuma was evaluated using numerical modelling. Numerical modelling provides a controlled and replicable means of testing how alternative defensive strategies perform under different tsunami source conditions and projected SLR scenarios. This approach enables systematic comparison of the overall effectiveness of each design and their capacity to sustain protection as baseline sea levels change. The focus on multi-layered defences reflects recognition that a single structural element is rarely sufficient to manage tsunami risk effectively. Instead, combinations of primary and secondary measures, designed with differing priorities such as durability, visual integration, and accessibility, can work together to reduce inundation, maintain the usability of the coast, and respond to evolving environmental conditions. Insights from community preferences, post-GEJE reconstruction plans, and existing literature on coastal defence performance were used to guide the conceptual development of new human centred multi-layered defence configurations. These designs were then assessed through numerical simulations to quantify their technical performance.

3.1 Conceptional Basis and Design Rationale

Tsunami mitigation in Japan has traditionally centred on large, single-purpose structures such as seawalls and breakwaters designed for hydraulic efficiency and structural strength. While these measures have reduced damage during moderate events, their limited adaptability and social acceptance have become increasingly evident since the GEJE. The national DRR framework now promotes multi-layered defence systems that combine several complementary measures to address both L1 and L2 tsunami. This study extends that framework by incorporating HCD principles into the conceptual development of multi-layered systems for Kesennuma, recognising that effective tsunami protection must balance engineering performance with the needs, perceptions, and everyday experiences of local communities. The rationale is that infrastructure designed to integrate with the environment and community identity is more likely to be maintained, trusted, and functionally sustainable under changing hazard conditions, including future SLR. The conceptual foundation for the designs presented in this study draws on three key elements: community-derived insights from Kesennuma, national reconstruction policy, and evidence

https://doi.org/10.5194/egusphere-2026-365
Preprint. Discussion started: 6 February 2026

from previous coastal engineering research. Results from Leggett et al. (2025) identified that residents valued visibility and openness to the sea, preferred defences that blended with the natural landscape, and expressed concern about excessive reliance on rigid concrete structures. However, the same study also showed that residents were divided about the sense of protection created by existing defences, with roughly equal proportions reporting that they did and did not feel secure behind the new seawalls. This divergence highlights the importance of evaluating whether different configurations, ranging from socially aligned to more structurally dominant, can achieve both technical reliability and community confidence. These social preferences were translated into engineering design principles that emphasised three priorities: (1) environmental integration through use of vegetated or low-impact elements, (2) unobtrusive protection that maintains visual and physical access to the waterfront, and (3) robust structural safety capable of withstanding rare, large-magnitude events.

Together, these priorities form the conceptual rationale for evaluating whether designs informed by community perspectives can achieve equivalent or superior technical performance compared with conventional configurations. The study therefore developed three conceptual multi-layered defence systems, each representing one of the priorities above. These configurations were not intended as construction plans but as analytical prototypes for quantitative assessment. By modelling their physical performance under present and future SLR conditions, the research examines the relationship between social preference and engineering effectiveness within a human centred tsunami protection framework. The following section describes the structure and composition of each system in detail, outlining how individual components and materials were combined to create integrated, testable configurations.

3.2 Alternative Multi-Layered Infrastructure

Developing tsunami mitigation systems that balance structural performance with social, environmental, and aesthetic considerations remains a major challenge for Japanese coastal cities. Following the GEJE, reconstruction highlighted both the strengths and limitations of hard-engineered measures such as seawalls and offshore breakwaters. While effective in reducing inundation and direct wave impacts (Suppasri et al., 2013; Strusińska-Correia, 2017), these defences have been criticised for their scale, cost, and lack of adaptability under future SLR scenarios. Their rigid designs often restrict visibility and coastal access, reducing public acceptance and disrupting the character of the waterfront (Oetjen et al., 2022; Aoki, 2018). Consequently, recent research and DRR policy have promoted multi-layered configurations, combining complementary offshore, coastal, and inland measures to distribute protective functions and improve resilience when individual layers are overtopped or damaged (Takabatake et al., 2020; Omori et al., 2019).

The designs developed in this study were guided by three sources: (1) community-derived preferences from Leggett et al. (2025), (2) evidence from peer-reviewed research confirming the prior use and tested effectiveness of each structural element, and (3) the principles of Kesennuma City's Disaster Recovery Plan, which emphasises 'harmony with nature' and 'community-focused planning to ensure that infrastructure aligns with both environmental and civic goals'. This integration ensures that the proposed systems are not reproductions of previous studies, but novel configurations created specifically for the Kesennuma context. Each design combines proven components to reflect one of three distinct priorities identified in

https://doi.org/10.5194/egusphere-2026-365
Preprint. Discussion started: 6 February 2026

Section 2.1: environmental integration, unobtrusive protection, and maximum structural protection. Each configuration includes offshore, coastal, and inland elements selected to perform complementary functions within Kesennuma's topography and urban structure. Construction and maintenance costs were not considered during the design process, as the focus was on conceptual performance and comparative effectiveness rather than financial feasibility. The layouts of the three designs, including component locations, elevations, and Manning's coefficients, are shown in Fig. 3 to Fig. 5.

3.2.1 Defence Design 1: Eco-Hybrid System (Environmentally Focused)

This configuration integrates natural and low-impact solutions to provide tsunami mitigation while maintaining ecological value and landscape continuity (Fig. 3). Offshore, submerged concrete pile arrays combined with artificial reef structures reduce wave energy through drag and turbulence while enhancing biodiversity (Strusińska-Correia, 2017). Along the coastline, narrow vegetated berms and bioswales act as secondary buffers that absorb overflow, filter sediment, and blend visually with the urban edge (Takabatake et al., 2020). Inland, elevated evacuation landscapes and urban green spaces create

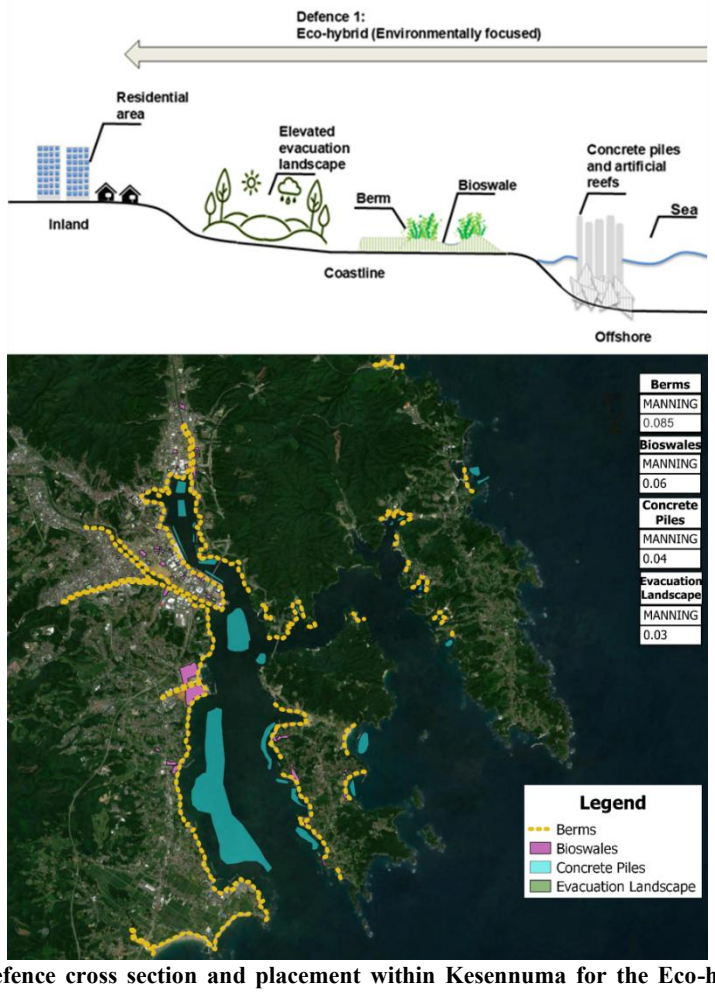

Fig. 3: Multi-layered defence cross section and placement within Kesennuma for the Eco-hybrid defence system (Defence 1). Base from Sentinel-2 imagery, Copernicus Programme, European Union.

https://doi.org/10.5194/egusphere-2026-365
Preprint. Discussion started: 6 February 2026

tertiary protection layers that function as both safe zones and daily-use public areas (Omori et al., 2019). This system tests whether ecologically sensitive, visually integrated designs can sustain tsunami protection under future SLR conditions while aligning with Kesennuma's emphasis on harmony with nature.

3.2.2 Defence Design 2: Discreet Integrated Barrier System (Unobtrusive and Open)

This configuration prioritises openness and visibility, minimising the psychological sense of separation from the sea (Fig. 4). Offshore, low-crest tetrapod fields are placed in a staggered grid to dissipate energy before waves reach the shore without creating strong visual obstruction. At the coastal interface, glass-composite seawalls with automated hydraulic floodgates provide transparency and adaptive protection in urban areas (Strusińska-Correia, 2017). These gates remain flush with the ground under normal conditions and elevate automatically during tsunami alerts. Inland, rooftop safe zones and elevated pedestrian pathways provide continuity of access and vertical evacuation options connected to key public buildings. This

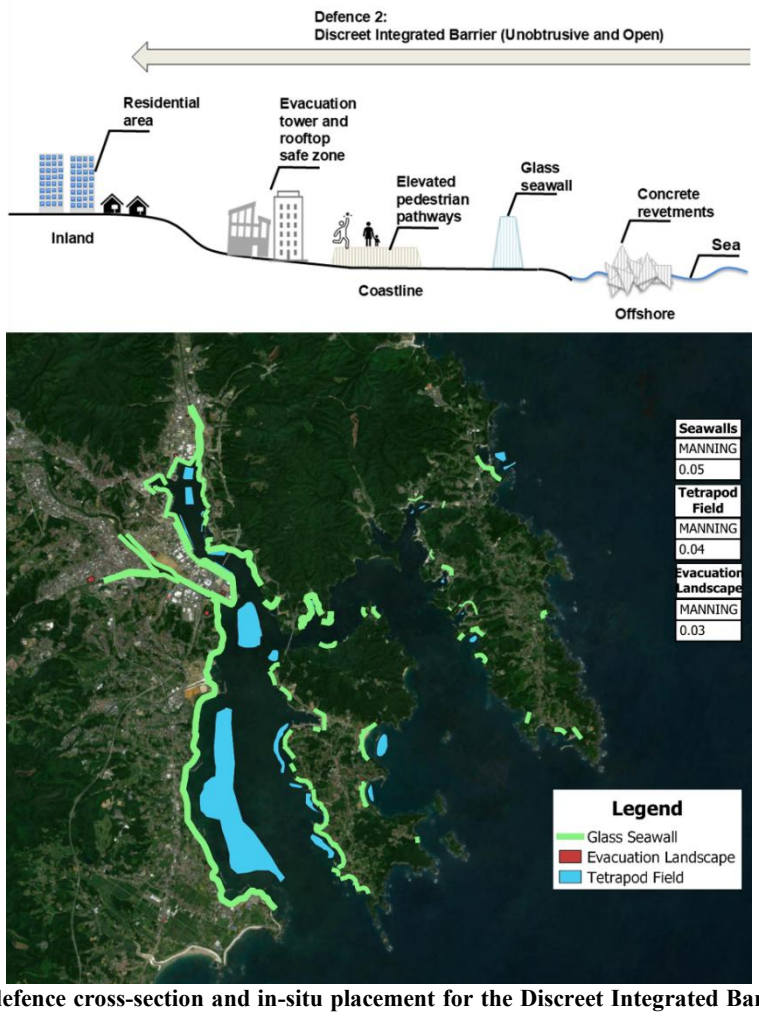

Fig. 4: Multi-layered defence cross-section and in-situ placement for the Discreet Integrated Barrier system (Defence 2). Base from Sentinel-2 imagery, Copernicus Programme, European Union.

https://doi.org/10.5194/egusphere-2026-365
Preprint. Discussion started: 6 February 2026

design evaluates whether maintaining open sightlines and physical connectivity to the waterfront can achieve acceptable tsunami mitigation performance while enhancing community acceptance and daily usability.

3.2.3 Defence Design 3: Reinforced High-Performance System (Maximum Structural Protection)

This configuration represents the most structurally focused of the three systems, providing a benchmark for maximum protection and redundancy (Fig. 5). Offshore, reinforced concrete pile fields are positioned around the harbour entrance to reduce resonance and limit surge penetration (Strusińska-Correia, 2017). Along the shoreline, stepped seawalls 5–7 m in height are paired with buffer parks that act as retention zones, temporarily storing overtopping water and reducing inland flow velocity (Takabatake et al., 2020). Further inland, floodable retention areas and channels provide controlled drainage and secondary containment (Omori et al., 2019). This design represents the engineering-led end of Kesennuma's mitigation

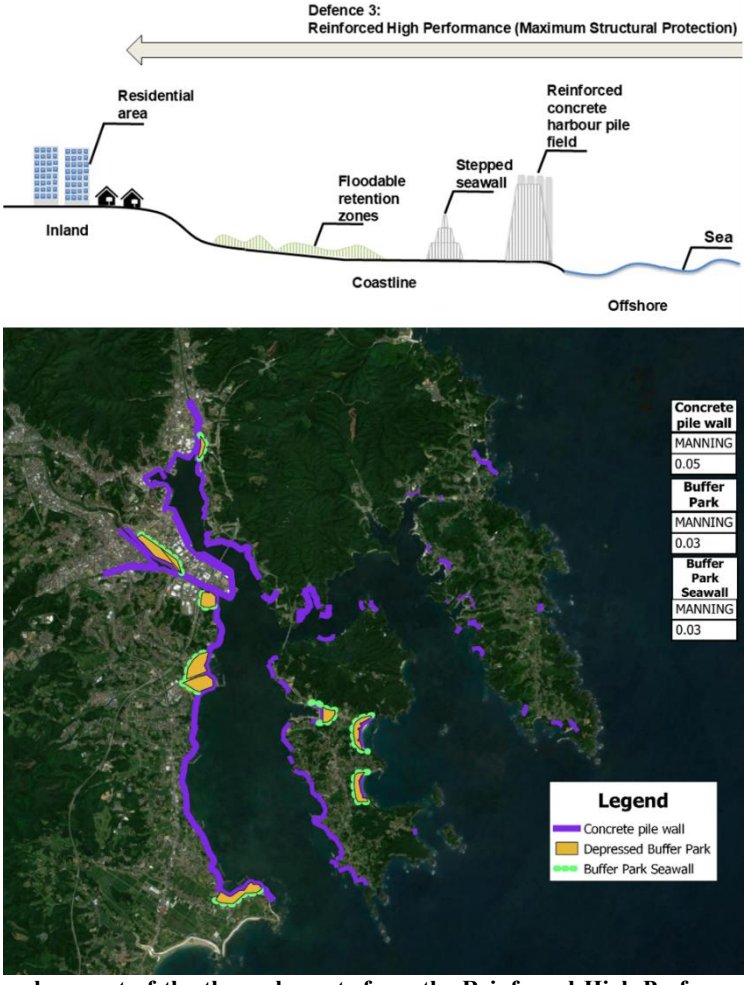

Fig. 5: Cross-section and in-situ placement of the three elements from the Reinforced High-Performance system (Defence 3). Base from Sentinel-2 imagery, Copernicus Programme, European Union.

https://doi.org/10.5194/egusphere-2026-365
Preprint. Discussion started: 6 February 2026

spectrum, testing the upper limit of structural performance against future SLR scenarios while allowing comparison with more socially aligned systems.

Together, these three configurations provide a structured basis for assessing how different design priorities influence inundation reduction and associated trade-offs. Each represents a distinct, yet technically feasible system developed from validated precedent studies, community insight, and local reconstruction principles. Collectively, they form the foundation for quantitative modelling and performance evaluation within a human centred tsunami protection framework.

3.3 TUNAMI-N2 Numerical Model

Tsunami propagation and inundation in Kesennuma City were simulated using TUNAMI-N2, a two-dimensional nonlinear shallow-water model that solves the depth-averaged nonlinear shallow-water equations (NSWE) for incompressible flow under the hydrostatic assumption (Imamura, 1996; Imamura et al., 2006). The model conserves mass and momentum in the horizontal plane and represents bottom friction through a spatially varying Manning coefficient (Imamura & Imteaz, 1995). The governing equations are:

Eq. (1) Continuity (mass conservation) :

$$\frac{\partial \eta}{\partial t} + \frac{\partial M}{\partial x} + \frac{\partial N}{\partial y} = 0 \quad (1)$$

Eq. (2) x-momentum:

$$\frac{\partial M}{\partial t} + \frac{\partial}{\partial x}\left(\frac{M^2}{D}\right) + \frac{\partial}{\partial y}\left(\frac{MN}{D}\right) = -gD\frac{\partial \eta}{\partial x} - gn^2\frac{M\sqrt{M^2+N^2}}{D^{7/3}} \quad (2)$$

Eq. (3) y-momentum:

$$\frac{\partial N}{\partial t} + \frac{\partial}{\partial x}\left(\frac{MN}{D}\right) + \frac{\partial}{\partial y}\left(\frac{N^2}{D}\right) = -gD\frac{\partial \eta}{\partial y} - gn^2\frac{N\sqrt{M^2+N^2}}{D^{7/3}} \quad (3)$$

where η is the free-surface elevation, M and N are the depth-integrated discharge fluxes in the x- and y-directions respectively, $D = \eta + h$ is the total water depth, h is the still-water depth, g is gravitational acceleration, and n is the spatially varied Manning roughness coefficient. The nonlinear friction terms represent bed shear stress, which dissipates flow momentum and controls near-shore velocity, inundation depth, and run-up.

The equations are solved using a staggered leap-frog finite-difference scheme that achieves second-order accuracy in both space and time while maintaining numerical stability in regions of rapid flow variation (Goto & Ogawa., 1997). Nonlinear advection terms are approximated using second-order central differences at interior nodes and first-order upwind differences near boundaries. A uniform time step of 1 s is used to satisfy the Courant–Friedrichs–Lewy (CFL) stability condition across all nested grids. Open boundaries apply radiation conditions to allow outgoing waves without reflection, and reflective boundaries are applied along impermeable coastal structures.

https://doi.org/10.5194/egusphere-2026-365
Preprint. Discussion started: 6 February 2026

TUNAMI-N2 has been extensively validated for tsunami propagation, run-up, and inundation in Japan, including applications along the Sanriku coast that share the complex topography and narrow bays characteristic of Kesennuma (Sugawara and Goto, 2012; Suppasri et al., 2013; Imamura et al., 2001). Reported mean absolute errors are typically below 10 % for inundation depth and extent when compared with observed data, confirming the model's reliability in environments of similar geometry and scale. Given this prior validation, the present study employs the same TUNAMI-N2 framework, spatial resolution hierarchy, and parameterisation approach to evaluate relative performance differences among defence configurations. The model is therefore used not to replicate a specific historical event but to provide a consistent, controlled environment for comparing multi-layered defence scenarios under present and projected SLR conditions. This fit-for-purpose application ensures that the modelling results are robust for assessing comparative trends in inundation behaviour and mitigation effectiveness in Kesennuma's coastal setting.

3.3.1 Computational Domain and Nested Grids

The computational domain covered the northern Tohoku region of Japan (37.8° N – 44.0° N, 140.8° E – 144.5° E), encompassing the Sanriku coast, Kesennuma City, and the full rupture areas of the fault sources considered (Fig. 6). Model coordinates and figure locations are expressed in metres using the Japan Plane Rectangular Coordinate System (Zone IX), providing a consistent georeferencing framework. This extent ensures that tsunami generation, offshore propagation, and nearshore transformation processes are all captured within a single consistent framework.

A six-layer nested grid system was implemented to resolve tsunami dynamics from offshore sources to detailed inundation within the urban environment. Grid resolutions ranged from 1,215 m in the outermost layer to 5 m in the innermost, with intermediate layers of 405 m, 135 m, 45 m, and 15 m. The innermost domain consisted of two 5 m grids: one covering Central Kesennuma, including the dense urban core and adjacent low-lying districts, and another extending across Kesennuma Bay, incorporating the Karakuwa Peninsula and surrounding coastal neighbourhoods. Coarser grids simulated regional propagation and wave dispersion across the wider bathymetry, while the 5 m grids resolved urban streets, river mouths, ports, and coastal slopes where run-up and inundation occur. This configuration provided the spatial precision needed to capture localised flow dynamics while maintaining computational efficiency across multiple simulation scenarios.

Bathymetric and topographic data were obtained from the high-resolution composite DEM developed by Sugawara, Takahashi and Imamura (2014), originating from the foundational Sanriku bathymetry and topography compilation by Takahashi et al. (2000). These datasets provide pre-2011 terrain for the Sanriku coast and represent the natural coastal and floodplain morphology prior to reconstruction. They were selected to ensure that the model evaluates new defence designs against a consistent pre-reconstruction baseline. Elevations were standardised to a mean sea level datum to maintain consistency with SLR scenarios. Reflective boundaries were applied along solid coastal structures, such as seawalls and revetments, while open boundaries used radiation conditions to allow outward wave propagation. Coastal defences, river embankments, and terrain features were incorporated directly into the digital elevation model, ensuring their effects on wave propagation, refraction, and overtopping were dynamically represented.

https://doi.org/10.5194/egusphere-2026-365
Preprint. Discussion started: 6 February 2026

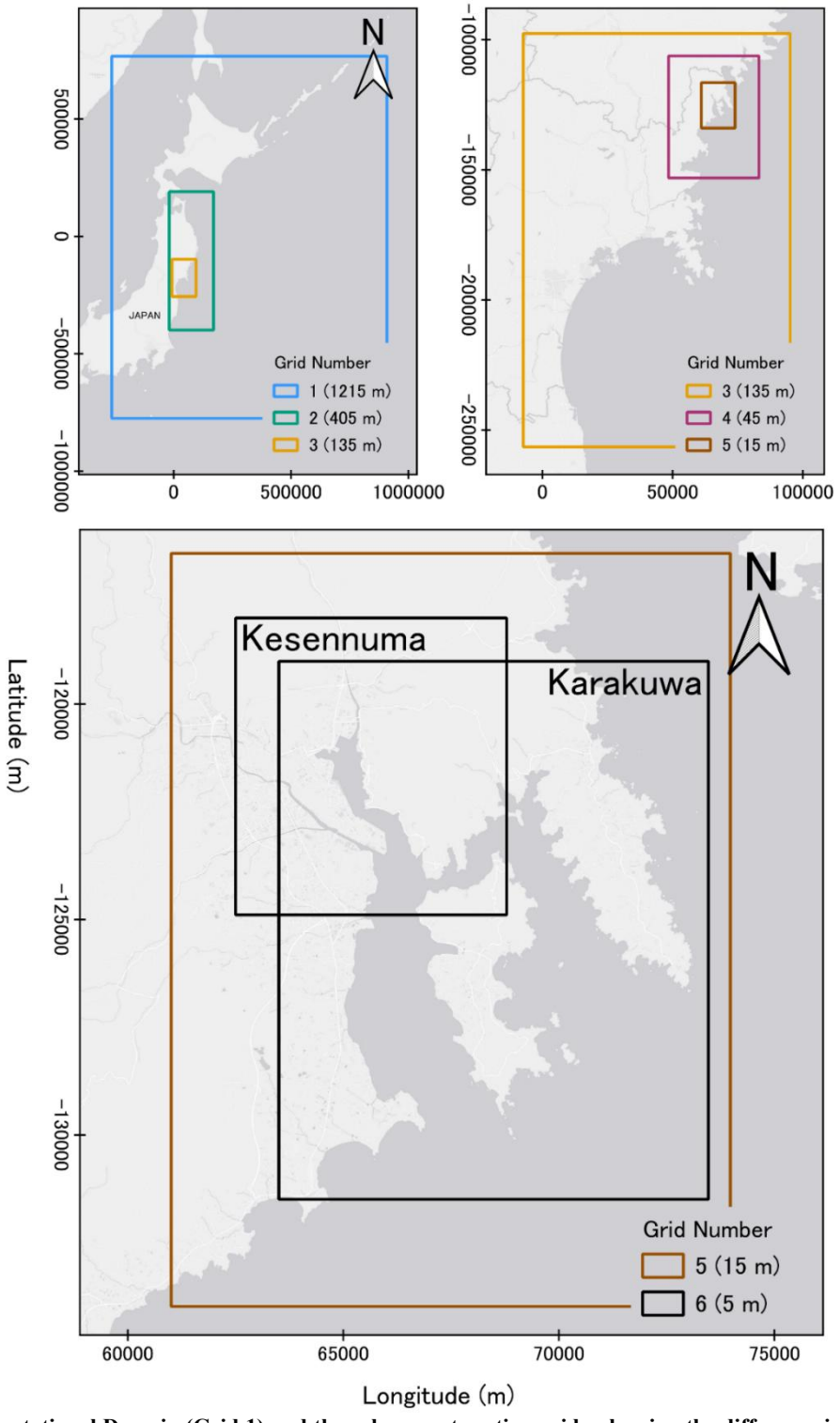

Fig. 6: Computational Domain (Grid 1) and the subsequent nesting grids, showing the difference in locations of the Kesennuma and Karakuwa final grids. Sources: Esri (World Gray Canvas) | Powered by Esri.

https://doi.org/10.5194/egusphere-2026-365
Preprint. Discussion started: 6 February 2026

3.3.2 Tsunami Source Models, Boundary Conditions and SLR Scenarios

Three tsunami source models were implemented to represent the main regional subduction zones that influence Kesennuma: the Kuril Trench, the Japan Trench, and the 2011 GEJE (Tohoku) source (). These correspond to the official three-fault framework used in Kesennuma City's hazard mapping and national Cabinet Office tsunami assessments. Fault parameters for the Kuril and Japan Trench scenarios were obtained from the Cabinet Office (2020), while the 2011 GEJE source parameters were taken from Satake et al. (2013). Okada (1985) dislocation theory was then applied to each subfault to compute seafloor deformation, providing the rupture geometry and vertical displacement associated with each event type. Together, these sources represent major megathrust earthquakes which, despite occurring in different locations, have demonstrated or are expected to produce tsunamis with significant impacts on Kesennuma. Each model was selected and implemented to produce representative maximum wave heights along the Sanriku coast, allowing meaningful comparison between scenarios.

Boundary conditions were applied according to the standard TUNAMI-N2 configuration. Open ocean boundaries used radiation conditions to allow outgoing wave energy to exit the domain without reflection, ensuring numerical stability during offshore propagation. Reflective boundary conditions were imposed along impermeable coastal structures to simulate wave impact and overtopping processes, while inland boundaries were treated as closed unless explicitly inundated. Grid interfaces between nested layers were linked through bilinear interpolation of surface elevations and discharge fluxes, conserving both mass and momentum during energy transfer from coarse to fine resolution grids.

SLR projections were incorporated into all simulations to represent changing baseline conditions. Two Shared Socioeconomic Pathways (SSPs) were used: SSP2–4.5, which represents the most probable mid-range warming and emissions trajectory under current global policy trends, and SSP5–8.5, which depicts a high-emissions, worst-case scenario. Local SLR projections for Kesennuma were obtained from the NASA Sea Level Projection Tool at the Ofunato II reference location with mean sea level increments of +0.40 m for 2050 and +0.97 m for 2100 applied for SSP2–4.5, and +0.44 m for 2050 and +1.28 m for 2100 for SSP5–8.5 (NASA, 2021). These increments were added to the still-water depth across all nested grids prior to simulation, modifying the baseline water level used by the model and influencing wave propagation, run-up, and inundation. No adjustments were made for vertical land movement.

https://doi.org/10.5194/egusphere-2026-365
Preprint. Discussion started: 6 February 2026

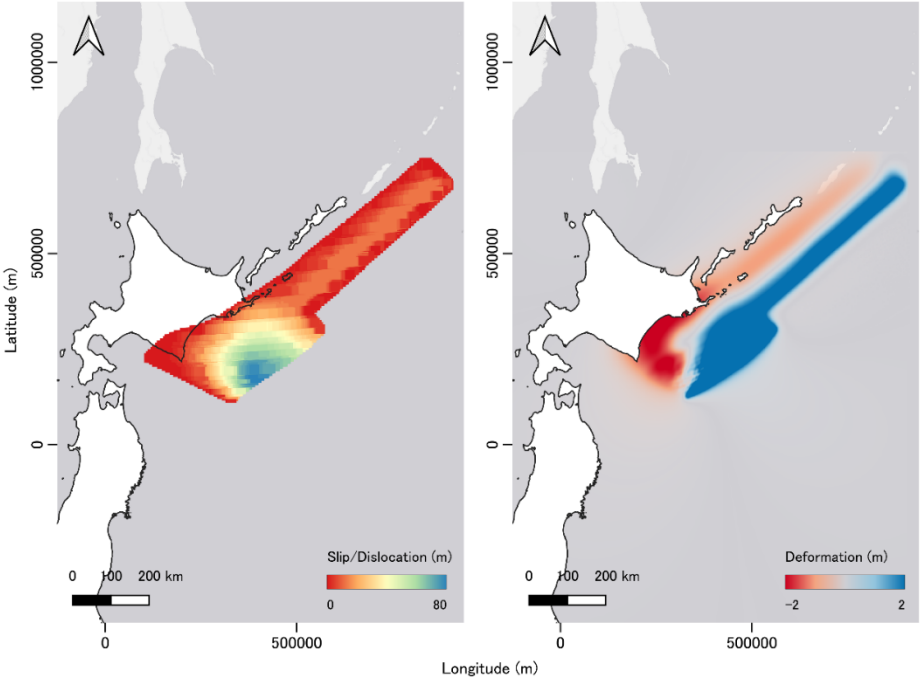

(a)

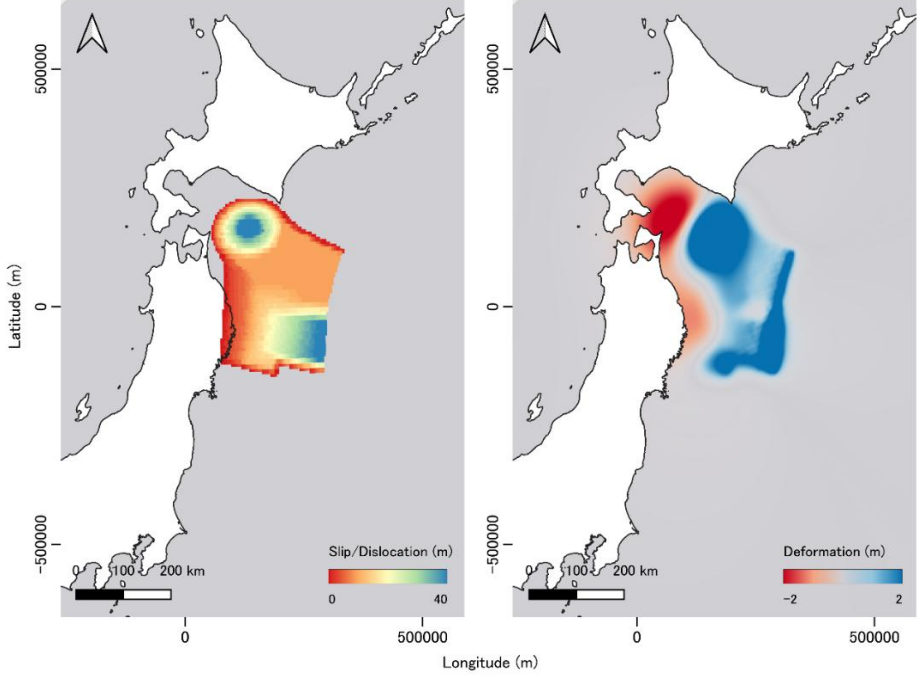

(b)

https://doi.org/10.5194/egusphere-2026-365
Preprint. Discussion started: 6 February 2026

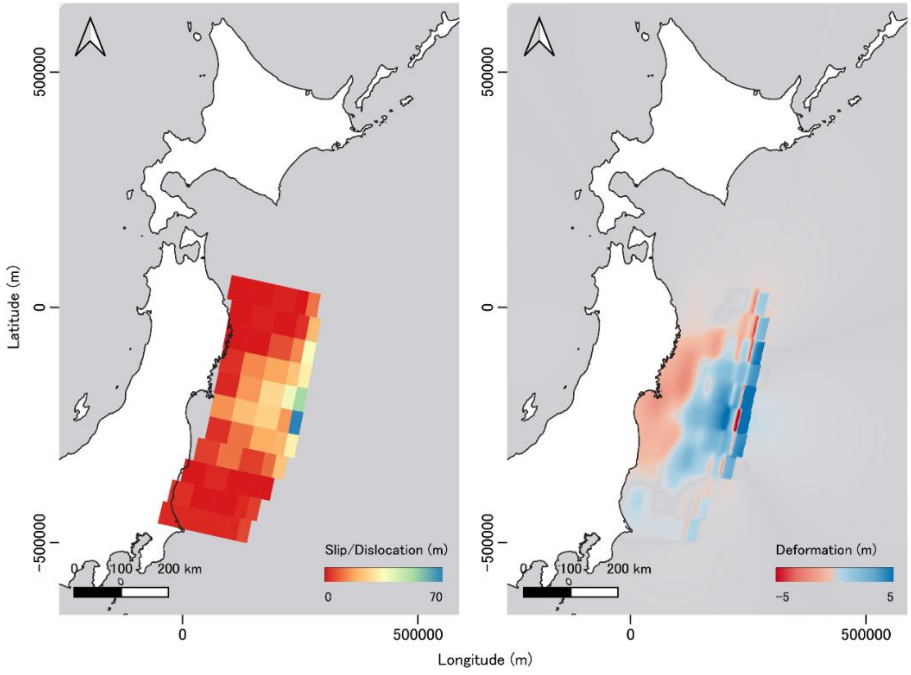

(c)

Fig. 7: Tsunami source model locations, slip distribution and deformation for (a) Kuril Trench (b) Japan Trench and (c) 2011 GEJE (Tohoku).

3.3.3 Surface roughness and Manning Coefficients

Spatially varied Manning's coefficients were applied to represent differences in surface roughness associated with land cover and coastal infrastructure. Land-cover data were obtained from the ESA WorldCover 2020 dataset via Google Earth Engine and reclassified to a 5 m resolution grid to match the innermost computational domains (Zanaga et al., 2021). The default classification was then replaced with a custom land-cover dataset developed for this study to ensure that surface categories accurately represented the physical and built conditions across Kesennuma's coastal plain. Manning's coefficients and their corresponding surface types were derived from established literature, including Bricker et al. (2015), Chow (1959), FEMA (2007), Yanagisawa et al. (2009), Yeh et al. (2012), and USACE HEC-RAS (2020). These sources were used to capture realistic variability across open water, beaches, vegetation, and urbanised areas. The coefficients listed in Table 1 were applied consistently across all simulations, including both present and future SLR conditions, so that variations in model results could be attributed to differences in water level or defence configuration rather than to changes in surface roughness. Frictional resistance was therefore the primary factor influencing nearshore flow velocity, wave attenuation, and inundation depth. This configuration follows established practice in tsunami inundation modelling and remains consistent with validated applications of TUNAMI-N2.

https://doi.org/10.5194/egusphere-2026-365
Preprint. Discussion started: 6 February 2026

Surface Type / Material	Mannings *n* Value	Source
Open water (deep ocean or smooth bay)	0.010 – 0.020	Bricker et al. (2015); Chow (1959)
Sandy beach / flat bare ground	0.015 – 0.025	Bricker et al. (2015); USGS WSP 2339
Short grass / maintained lawn	0.025 – 0.035	Bricker et al. (2015); Chow (1959)
Long grass / wild vegetation	0.040 – 0.050	Bricker et al. (2015); USGS WSP 2339
Shrubs / low bushes	0.050 – 0.080	Bricker et al. (2015); FEMA (2007)
Dense forest / coastal forest	0.080 – 0.150	Bricker et al. (2015); FEMA (2007)
Urban areas (residential, buildings)	0.050 – 0.120	Bricker et al. (2015); Goto et al. (2009); Yeh et al. (2012)
Urban roads / paved areas	0.020 – 0.030	USACE HEC-RAS (2020)
Concrete seawall / revetment crest	0.015 – 0.030	Bricker et al. (2015); Goto et al. (2009)
Rubble mound revetment (rough crest)	0.040 – 0.060	Bricker et al. (2015)
Reinforced glass / thick Perspex (smooth)	0.009 – 0.013	USACE HEC-RAS (2020); Engineering Toolbox (2000)

Table 1: Mannings coefficient value ranges and their sources used in this study. Unless otherwise shown in the figures for each defence system, values were typically taken from the midpoint of these ranges.

3.4 Simulation set-up and Outputs

A total of 150 simulations were conducted to evaluate the performance of alternative multi-layered tsunami defence configurations under varying source and SLR conditions. The simulations covered all combinations of two study areas (Central Kesennuma and the Karakuwa Peninsula), three tsunami sources (Kuril Trench, Japan Trench, and GEJE), five defence scenarios (no defences, current defences, and the three proposed multi-layered designs), and five SLR conditions (current, plus SSP2–4.5 and SSP5–8.5 for 2050 and 2100). This structure enabled systematic comparison across both present and projected conditions while isolating the influence of defence configuration and sea level.

Each simulation produced a complete set of spatial and temporal outputs stored as georeferenced raster datasets. The resulting data were subsequently analysed to derive quantitative indicators representing the physical and human dimensions of tsunami impact under different hazard and defence conditions. These outputs provide the foundation for the subsequent assessment of inundation extent, fatality rate, and economic loss, which together capture the combined physical and social performance of the tested defence systems. The following sections describe in detail the procedures used to calculate each of these indicators from the model results.

https://doi.org/10.5194/egusphere-2026-365
Preprint. Discussion started: 6 February 2026

3.4.1

Inundation extent represents one of the most fundamental indicators in tsunami hazard assessment, providing a direct, spatially quantifiable measure of the total area flooded during a tsunami event. It serves as a first-order metric of hazard intensity and potential exposure, enabling comparison of the relative protective capacity of different coastal defence configurations.

For each simulation, inundation extent was calculated from the model output by summing the total area of all grid cells in which water depth values were positive. This method captures spatial variation in flooding and provides a single aggregated value for each scenario. The calculation followed Eq. (4):

$$A = \sum_{i,j}(\Delta x\, \Delta y), \quad \text{for all cells where } h_{i,j} > 0 \tag{4}$$

where $h_{i,j}$ represents the water depth at grid cell (i, j), and Δx and Δy are the dimensions of each cell in metres. A minimum depth threshold of 0.01 m (1 cm) was applied to define inundation. This threshold does not represent physically significant flooding but serves to exclude minor numerical oscillations and residual wetting inherent to finite-difference tsunami solvers. Similar small thresholds have been adopted in previous tsunami modelling studies to stabilise wet–dry interfaces and maintain computational accuracy (Imamura, 1996; Goto et al., 1997).

This cell-based approach preserves the fine-scale variability of inundation patterns across Kesennuma's coastal plain and allows consistent aggregation at the city scale. By applying the same computational domain and grid resolution across all scenarios, the resulting inundation areas can be directly compared to assess the effect of different defence designs.

The use of total inundated area as a comparative measure is well supported in tsunami research, having been shown to correlate strongly with flow depth, run-up, and structural damage in both empirical and model-based studies (Shuto & Fujima, 2009; Shigihara et al., 2022). Comparing inundation areas between identical source and SLR conditions isolates the influence of defence design, allowing reductions in flooded area to be interpreted as direct indicators of mitigation effectiveness. This provides a reproducible and transparent basis for evaluating how each defence configuration contributes to overall hazard reduction.

3.4.2 Fatality Rates

Fatality estimation provides a quantitative measure of potential human loss and is an essential indicator in tsunami risk assessment. It links physical hazard intensity to population exposure, allowing evaluation of how changes in defence configuration alter potential casualties. For this study, fatalities were estimated using depth based empirical fatality rates derived from observed tsunami impacts. Population data were obtained from the official 500 m Japanese census mesh. Census counts were transferred to the 5 m tsunami model grid using an areal weighting, population conserving redistribution approach. For each 500 m census cell, population density was assumed to be spatially uniform within the cell. The total population of each census cell was therefore distributed across all intersecting 5 m tsunami grid cells in proportion to the fraction of the census cell area covered by each 5 m cell. This ensured that population totals were exactly preserved while

https://doi.org/10.5194/egusphere-2026-365
Preprint. Discussion started: 6 February 2026

enabling population exposure to be represented at the tsunami model resolution. For each grid cell, the modelled maximum water depth was used to assign a fatality rate based on depth ranges established in prior studies, shown in Table 2:

Depth	Fatality Rate
0–0.5 m	1%
0.5–2 m	10%
2–5 m	35%
5–10 m	60%
>10 m	80%

Table 2: Depth based fatality rates used in our fatality rates calculations adopted from empirical tsunami fatality functions consistent with Suppasri et al., (2016) and Koshimura et al., (2009b).

The depth thresholds and associated fatality probabilities used in this study are adopted from empirical tsunami fatality functions developed from analyses of the 2011 Tohoku event and are consistent with depth–mortality patterns reported in earlier tsunami vulnerability studies (Suppasri et al., 2016; Koshimura et al., 2009b). The estimated fatalities for a single computational mesh (F_i) are defined as the product of the exposed population and the depth-dependent fatality rate, as expressed in Eq. (5):

$$F_i = P_i \, x \, R(h_i) \quad (5)$$

where P_i represents the population count within mesh i, and $R(h_i)$ is the fatality rate derived from the specific inundation depth h at that location i. Finally, the total fatality count for the entire simulation area F_{total} was obtained by aggregating the values across all meshes (N) in the domain, as shown in Eq. (6):

$$F_{total} = \sum_{i=1}^{N} F_i \quad (6)$$

This method captures the non-linear relationship between inundation depth and mortality, which increases sharply with flow depth and velocity (Ishiguro & Yano, 2015; Suppasri et al., 2016). Field evidence from past tsunamis, including the 2011 Tohoku event, shows the same pattern: mortality rises rapidly once depths exceed approximately 2–3 m due to greater flow energy, debris loading, and reduced survivability (Koshimura et al., 2009b; Suppasri et al., 2016). Depth-based fatality models therefore provide a practical and empirically grounded method when detailed behavioural or evacuation data are unavailable. They have been applied successfully across multiple tsunami settings and magnitudes, demonstrating robust predictive capability for scenario-based risk assessment. By comparing fatality estimates across scenarios that share identical fault models, SLR conditions, and population distributions, any reduction in total or spatially distributed fatalities can be attributed directly to the influence of coastal defence design. This provides an interpretable, human centred measure of protective performance and complements the physical metrics of inundation and flow depth.

3.4.3 Economic Loss

Economic loss estimation translates physical damage into financial impact, providing an intuitive and policy-relevant measure of tsunami consequences. It complements physical hazard metrics by expressing results in economic terms that directly relate to reconstruction needs and fiscal risk. Building footprints for Kesennuma were obtained from OpenStreetMap

https://doi.org/10.5194/egusphere-2026-365
Preprint. Discussion started: 6 February 2026

(© OpenStreetMap contributors) using a BBBike.org extract, processed with osmium2shape to retain building polygons and clipped to the model domain. Attribute fields in the OSM dataset enabled identification of building use, allowing the separation of all buildings from key buildings. All features were converted to centroids and rasterised at 5 m resolution to align with the innermost computational grid.

Each building footprint was assigned a damage rate based on the maximum inundation depth calculated in the model outputs. The classification adopted in this study is seen in **Error! Reference source not found.** (after MLIT, 2013b; S uppasri et al., 2013; FEMA, 2015).

Depth	Damage Rate
<0.3 m	0%
0.3–1.0 m	20%
1.0–2.0 m	50%
>2.0 m	100%

Table 3: Depth based damage rates used within the study (after MLIT, 2013b; Suppasri et al., 2013; FEMA, 2015).

Per-building economic loss was then computed as Eq. (7)

$$\text{Economic Loss}_{\text{building}} = \text{Damage Rate} \times 20{,}000{,}000 \quad (7)$$

where ¥20,000,000 represents a single conservative proxy for building replacement cost (after Japan Cabinet Office., 2019; Tanikawa et al., 2017) . Although this represents a typical residential replacement cost, it is applied to all building types because Japanese government guidelines permit the use of a single representative asset value when detailed typology data are unavailable. This follows the approach adopted in rapid post-disaster loss accounting by the Cabinet Office (2019), where aggregated capital-stock values are applied uniformly in municipalities lacking structure-specific inventories, and in nationwide building-stock estimation methods such as Tanikawa et al. (2017), which use averaged unit construction costs across heterogeneous building stocks. MLIT flood-damage survey procedures likewise allow the application of unified asset values and depth–damage functions when structural categories cannot be reliably distinguished (MLITb, 2023). In Kesennuma, the coastal built environment is dominated by small-scale residential dwellings, making a residential proxy representative of most structures in the study area. Because non-residential and reinforced-concrete buildings generally have higher replacement costs than dwellings, applying a residential-scale proxy (¥20M) yields conservative loss estimates for mixed inventories. This remains consistent with MLIT and Cabinet Office practice, in which hazard intensity (e.g., inundation depth or seismic motion) drives variation in loss, while the monetary value of exposed buildings may be represented with a unified proxy when structural categories cannot be distinguished. Although OSM building footprints only provide basic typology tags rather than detailed structural information, the available building type data was sufficient for this study, and using per building footprints with depth-based loss functions remains suitable because variation in inundation depth contributes more to economic loss than structural characteristics in this modelling framework. Key buildings, including hospitals, schools, fire and police stations, designated evacuation facilities, and other critical service providers, were analysed separately using the same depth–damage classes and unit replacement cost; building distribution and the location of key buildings can be seen in Fig. 8. This allows targeted assessment of potential disruption to essential services

https://doi.org/10.5194/egusphere-2026-365
Preprint. Discussion started: 6 February 2026

and supports prioritisation of mitigation and recovery efforts beyond aggregate loss alone. Total citywide loss for each simulation was obtained as Eq. (8):

$$\text{Total Loss} = \sum_{i=1}^{N}(100\,\text{Damage Rate}_i \times 20{,}000{,}000) \quad (8)$$

A damage ratio was deliberately not used because averaging damage rates across all buildings collapses spatial and structural variation, removing the differentiation that the ratio is intended to represent. Economic loss calculations preserve this variation by maintaining per-building distinctions and provide a more interpretable expression of impact for both technical and public audiences. The combined use of total-building and key-building losses therefore provides both a system-level estimate of financial impact and a focused indicator of critical infrastructure vulnerability. By comparing economic losses across identical source, SLR, and location conditions, differences can be directly attributed to the presence and configuration of tsunami defences. This approach yields a transparent and reproducible basis for evaluating the cost-effectiveness of each multi-layered system, supporting both engineering optimisation and community-oriented resilience planning.

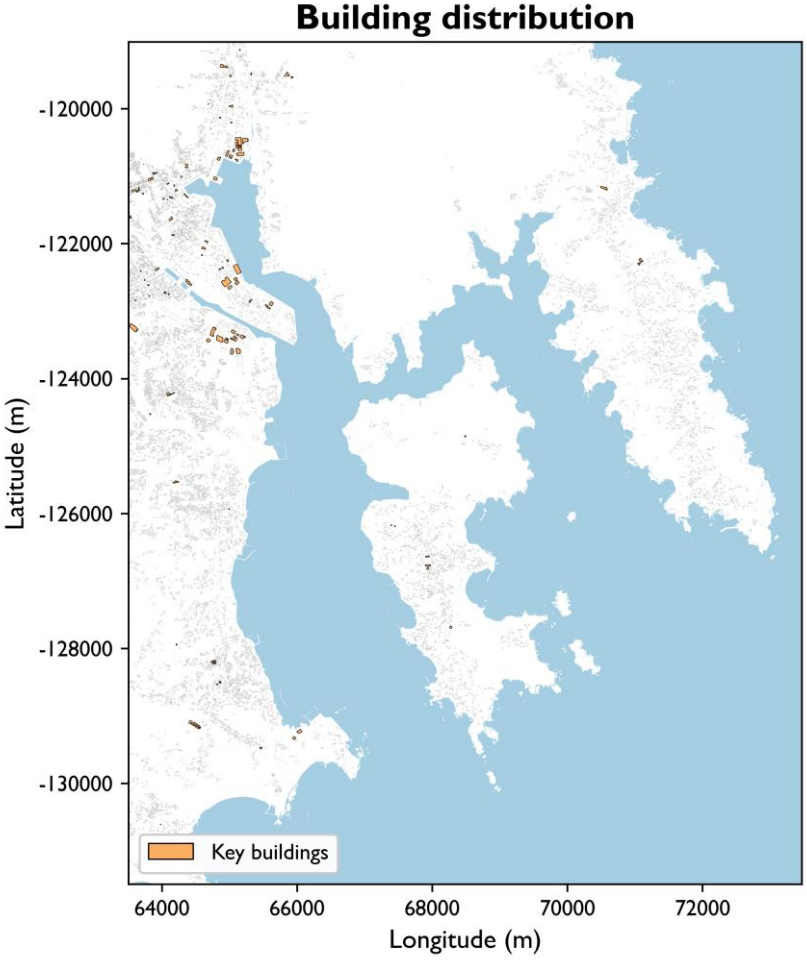

Fig. 8: Building distribution within Kesennuma, showing the location of Key Buildings such as hospitals, dentists and other health facilities, schools, government offices and utilities.

https://doi.org/10.5194/egusphere-2026-365
Preprint. Discussion started: 6 February 2026

4 Results

Building on the simulation framework described in Section 3, this section presents the outcomes of the TUNAMI-N2 modelling and subsequent analyses. The results evaluate how each multi-layered defence configuration performs across the modelled tsunami scenarios and SLR conditions. Outputs for inundation extent, fatality rate, and economic loss were derived from the numerical simulations and spatial post-processing described previously. Together, these indicators provide an integrated basis for assessing the physical, human, and economic performance of each defence system. All figures in the following results sections use outputs from the Japan Trench tsunami source as a representative case. Although the absolute magnitudes of inundation, fatalities, and economic losses differ between the three modelled source scenarios (Japan Trench, Kuril Trench, and GEJE), all sources produced the same relative performance hierarchy among the three defence configurations. The Japan Trench scenario therefore provides a clear and representative basis for illustrating spatial patterns and comparative differences between the defences without altering the conclusions drawn from the full multi-source dataset.

4.1 Sea level rise

Simulations show that tsunami inundation area and depth both increase progressively with rising sea levels under the SSP2–4.5 and SSP5–8.5 scenarios (Fig. 9). Across all simulations, higher SLR levels produced deeper and more extensive flooding, greater overlap between adjacent flood zones, and wider low-lying areas exposed to inundation. In Kesennuma, water depths increased most noticeably along inner bay margins, river corridors, and reclaimed coastal land, where even moderate SLR led to deeper and more continuous flooding. By 2100, particularly under SSP5–8.5, isolated shallow zones merged into a single, continuous inundation belt along the waterfront, with deeper pockets forming in enclosed basins and port areas. In Karakuwa, the effect of SLR was more pronounced, with both inundation depth and flooded area expanding substantially across the low-lying southern and eastern plains. Floodwaters penetrated further inland and maintained higher depths for longer durations, especially under late-century high-emission conditions. Overall, both study areas exhibited a consistent pattern of increasing inundation depth and total flooded area with SLR, with the most pronounced amplification occurring by 2100 under the SSP5–8.5 scenario.

https://doi.org/10.5194/egusphere-2026-365
Preprint. Discussion started: 6 February 2026

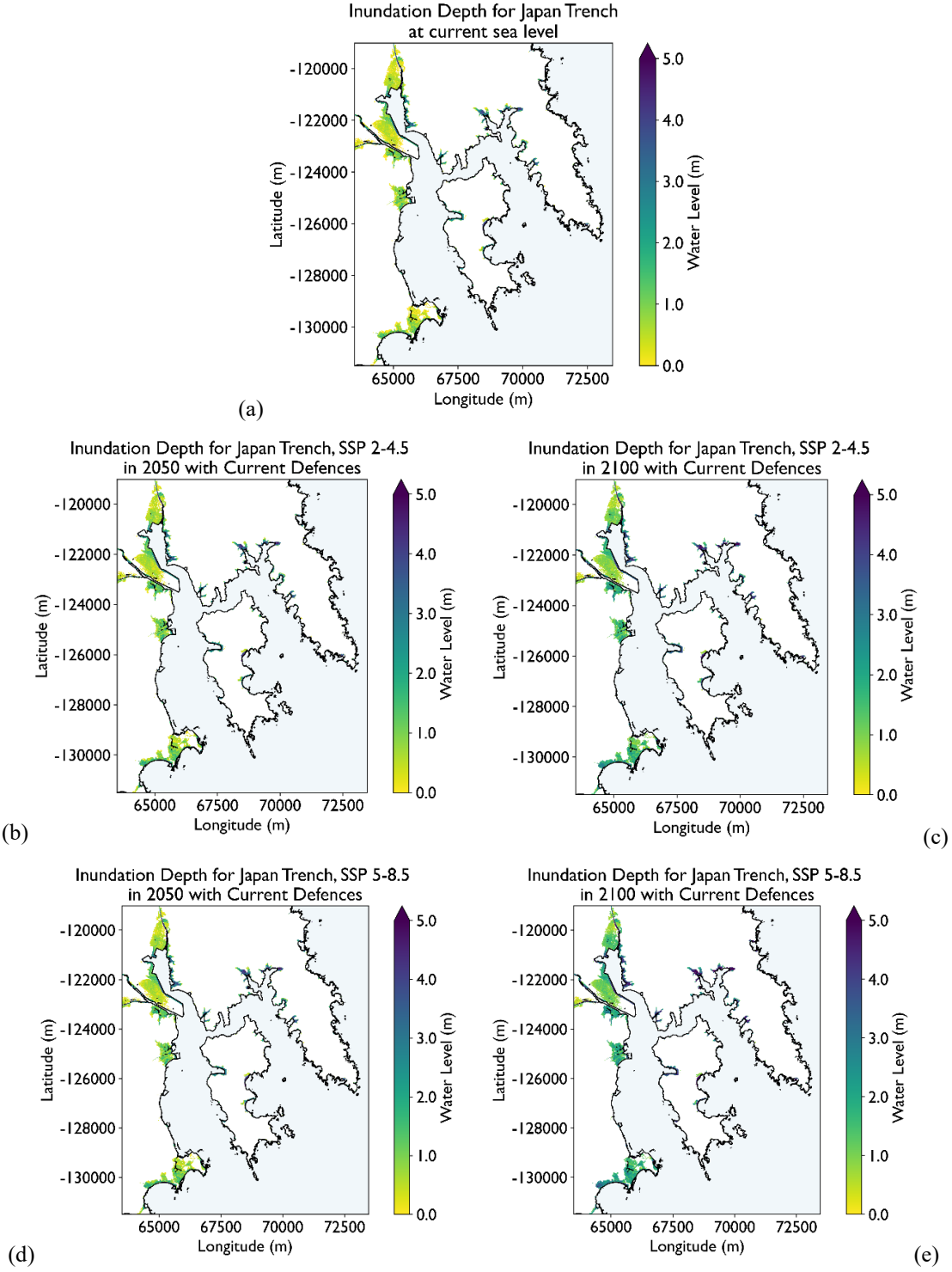

Fig. 9: Increasing inundation extent and depth under different SLR scenarios (a) No SLR, (b) SSP2-4.5 in 2050, (c) SSP2-4.5 in 2100, (d) SSP5-8.5 in 2050 and (e) SSP5-8.5 in 2100.

https://doi.org/10.5194/egusphere-2026-365
Preprint. Discussion started: 6 February 2026

4.2 Inundation Extent

Differences in inundation area and containment capacity between the three proposed multi-layered defence configurations are evident across all scenarios (**Error! Reference source not found.** to **Error! Reference source not found.**). Under cu rrent sea levels, all three designs substantially reduced flooding compared with the undefended baseline, demonstrating the effectiveness of layered protection. As SLR conditions intensified, however, the ability of each system to sustain protection diverged, revealing distinct performance hierarchies. Across both Kesennuma and Karakuwa, Defence 3 consistently achieved the strongest containment, limiting inland spread and maintaining smaller inundated areas. Defence 2 provided nearly equivalent performance, showing minor additional lateral propagation, while Defence 1 allowed broader, shallower flooding across low-lying terrain. These contrasts became more pronounced under high SLR scenarios, indicating that robust, continuous configurations retained protective capacity more effectively than softer or more permeable designs.

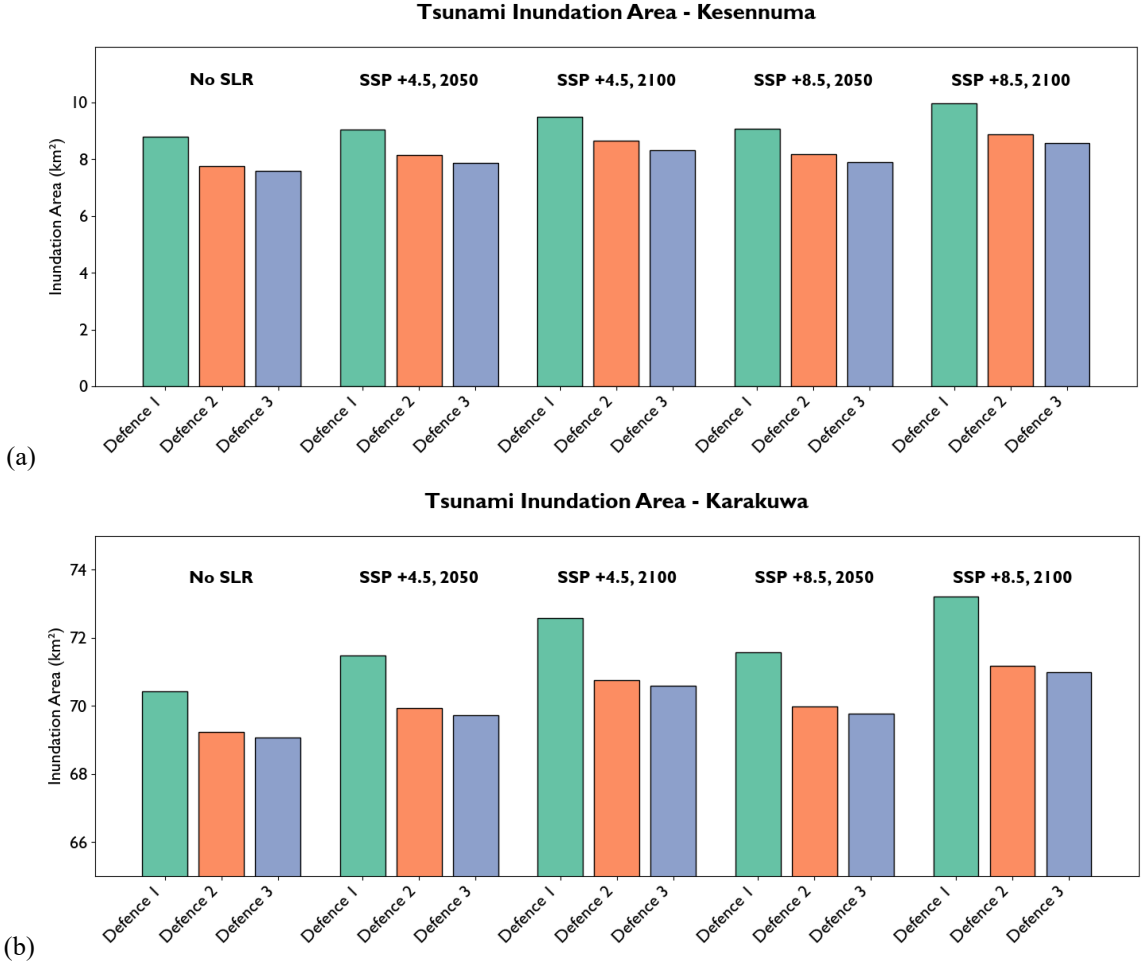

Fig. 10: Inundation area for (a) Kesennuma and (b) Karakuwa across all SLR scenarios for the three defence configurations, based on the Japan Trench tsunami source model. In both locations, inundation extent increases with SLR, with Defence 2 and Defence 3 limiting area more effectively than Defence 1.

https://doi.org/10.5194/egusphere-2026-365
Preprint. Discussion started: 6 February 2026

In Kesennuma, inundation under Defence 1 extended through urban corridors near the port and along transport routes, while Defence 2 and Defence 3 confined flooding largely to the immediate waterfront. Both reinforced systems preserved interior dry zones, even under late-century SLR, while the eco-hybrid design permitted shallow flooding across a wider area. In Karakuwa, Defence 3 restricted inundation to narrow coastal strips, maintaining clear separation between shoreline and inland settlements. Defence 2 performed similarly, though with slightly greater expansion along southern embayment's. Defence 1 produced the widest and most continuous flooding, especially where the vegetated berms and bioswales were overtopped. The spatial comparison map in Fig. 11 highlights these relationships. The blue zones (Defence 3) show the smallest inundation footprint, green (Defence 2) display moderate expansion, and orange (Defence 1) represent the broadest flood coverage. The consistency of this ranking across all SLR conditions confirms that defence configuration, rather than SLR alone is the principal determinant of inundation area and depth.

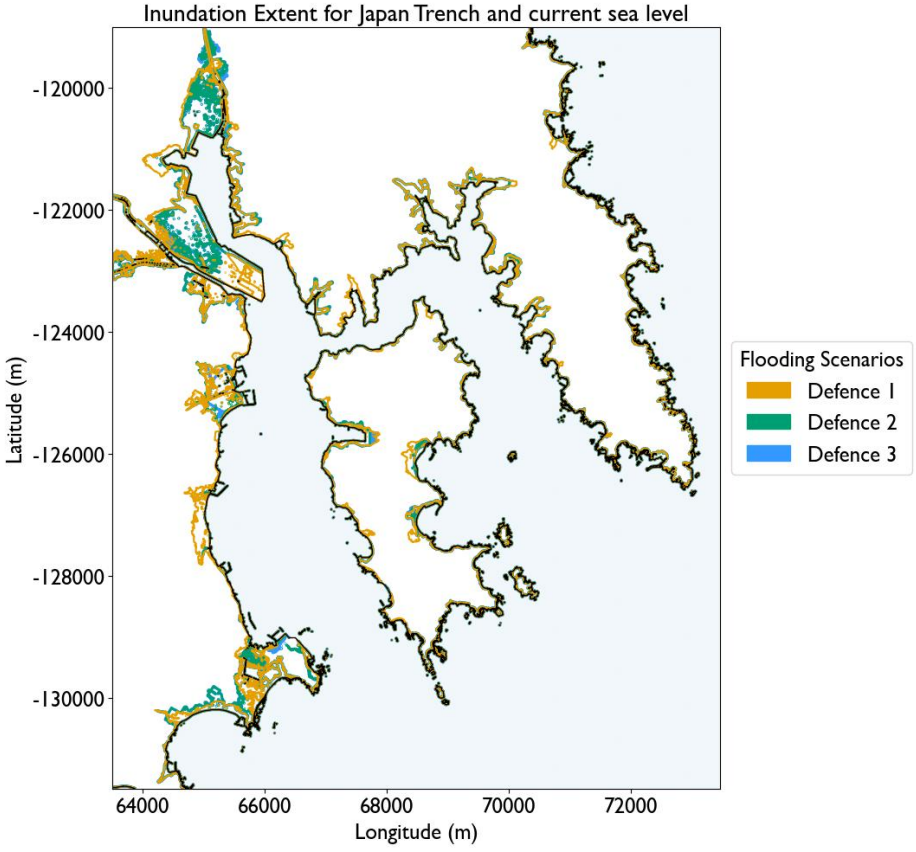

Fig. 11: Spatial extents showing differences in inundation patterns and areas for each defence configuration.

https://doi.org/10.5194/egusphere-2026-365
Preprint. Discussion started: 6 February 2026

4.3 Fatality Rate

Fatality estimates reflect clear spatial and structural patterns across the study area (Fig. 12). Overall, outcomes are governed primarily by the configuration and continuity of coastal defences, with SLR acting as a secondary influence on overall exposure.

In Kesennuma, all three defences perform similarly under present-day and mid-century (2050) conditions, with only marginal differences between SLR scenarios. By 2100, Defence 1 exhibits a noticeable rise in fatality rate under both SSP2–4.5 and SSP5–8.5, indicating reduced containment of inundation in the densely populated urban core. In contrast, Defence 2 and Defence 3 maintain almost identical fatality rates across all conditions, with negligible change or very slight decreases under late-century SLR. This pattern demonstrates stable performance of these two configurations under progressively elevated water levels, with no evidence of significant degradation over time. In Karakuwa, fatality rates remain low and largely unchanged across all SLR conditions for Defence 2 and Defence 3. For Defence 1, a very small increase is observed by 2100 under both SSP scenarios, but the change is minimal and remains within a narrow range. The limited variation across scenarios reflects the topographic control exerted by the peninsula's elevated terrain and the smaller extent of exposed settlement areas.

Across both sites, the results indicate a consistent structural hierarchy in human exposure outcomes. Defence 2 and Defence 3 maintain comparable and stable performance under all SLR conditions, while Defence 1 shows slightly reduced effectiveness only under late-century, high-emission scenarios. These trends demonstrate that the relative influence of SLR on fatality outcomes remains secondary to the configuration and continuity of coastal defences.

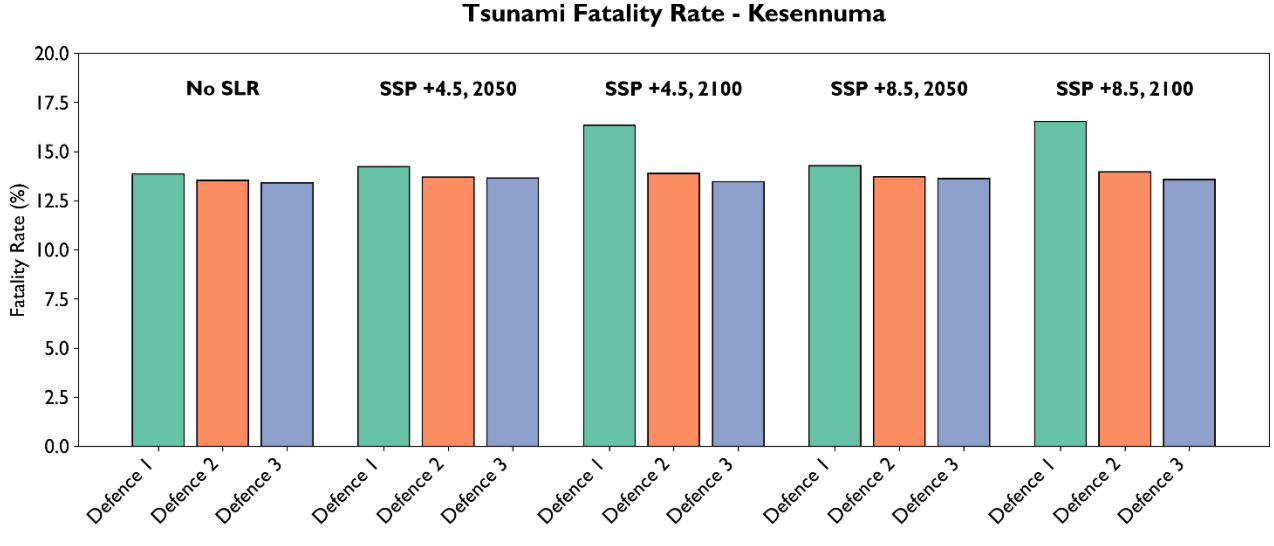

(a)

https://doi.org/10.5194/egusphere-2026-365
Preprint. Discussion started: 6 February 2026

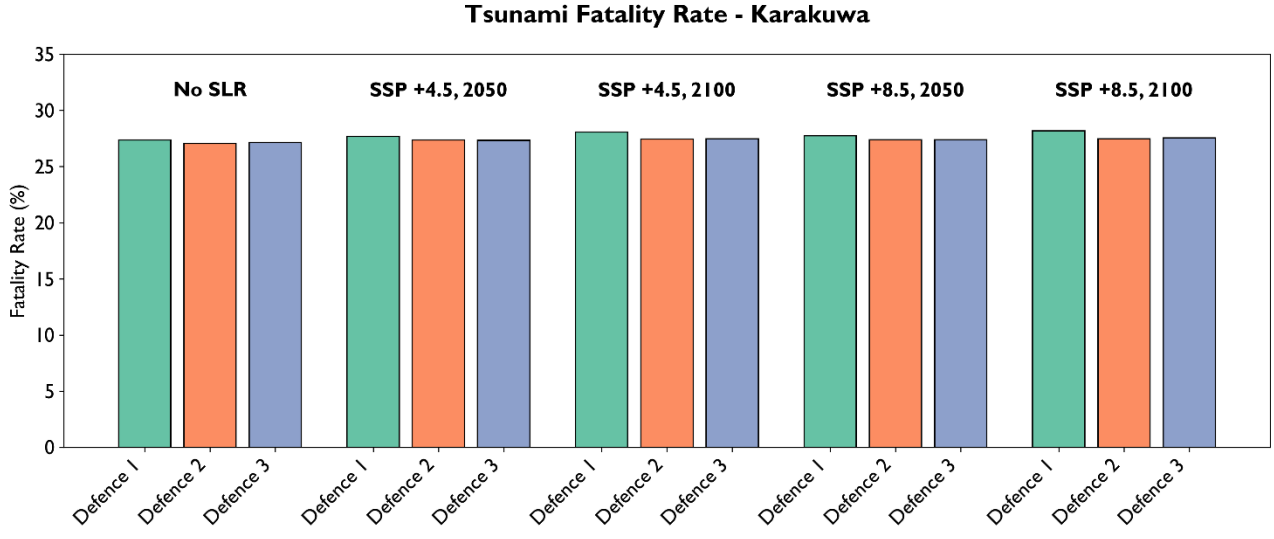

(b)

Fig. 12: Fatality estimates for the three defence configurations under all SLR scenarios for (a) Kesennuma and (b) Karakuwa, based on the Japan Trench tsunami source model. Fatality rates increase significantly at the highest sea level increase in Kesennuma, and the relative performance of the defences stays consistent throughout, although differences are marginal within Karakuwa.

4.4 Economic Loss

Patterns of economic loss further reinforce the structural hierarchy observed with SLR and inundation extent. Total losses for all buildings and key infrastructure increased under higher SLR, but the rate and magnitude of increase were strongly dependent on the defence configuration (Fig. 13 and Fig. 15). Across both study areas, Defence 3 consistently produced the lowest total and key-building losses, while Defence 2 achieved nearly comparable reductions. Defence 1 allowed significantly higher losses due to broader inundation and deeper flooding across developed areas. The largest differences between designs occurred under late-century SLR, highlighting that continuous, structurally reinforced systems maintain their performance advantage even as background water levels rise. In Kesennuma, economic losses were concentrated along waterfront districts, industrial areas, and river-mouth corridors. Defences 2 and 3 limited these losses primarily to shallow zones near the port, preventing inland spread and protecting critical facilities. Defence 1 reduced losses relative to the baseline but allowed wider low-intensity flooding, increasing the number of affected buildings despite lower individual damage levels. Fig. 14 illustrates the spatial distribution of economic loss per building under Defence 1 for the SSP5–8.5 scenario in 2100, representing the conditions with the largest overall losses across all simulations. Loss is seen around Kesennuma's port district, along the main waterways, and near river mouths and coastal margins where inundation depths are greater and building density is high. In contrast, little loss is evident in the more elevated and inland sectors, particularly outside the central urban basin, where topography limits flood penetration. The pattern shows that economic loss is concentrated in low-lying urban and estuarine zones around the port area, while inland and higher-elevation areas remain

https://doi.org/10.5194/egusphere-2026-365
Preprint. Discussion started: 6 February 2026

largely unaffected. Defences 2 and 3 display similar spatial distributions but with smaller affected areas and lower loss magnitudes.

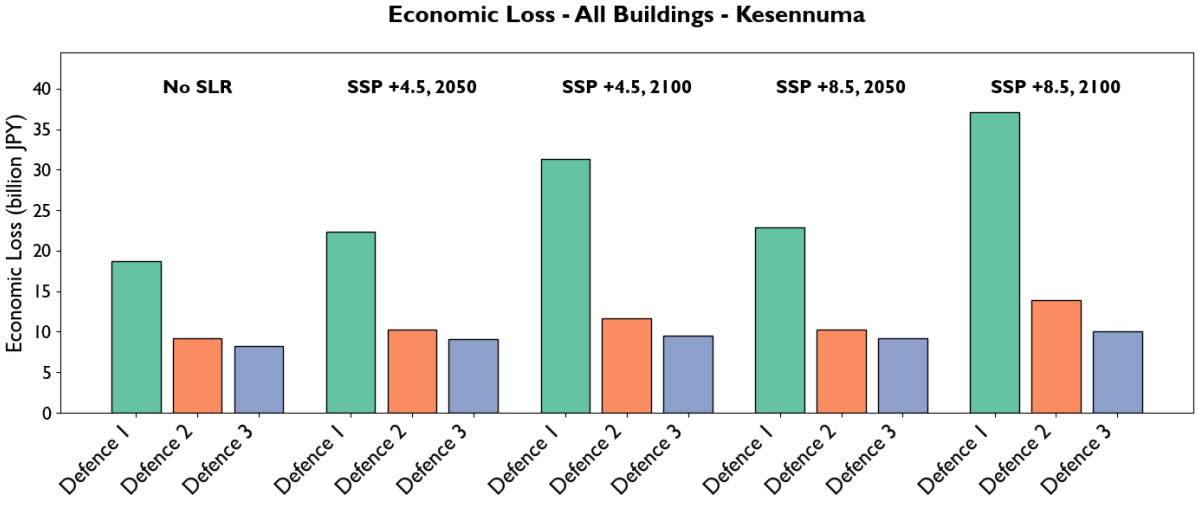

(a)

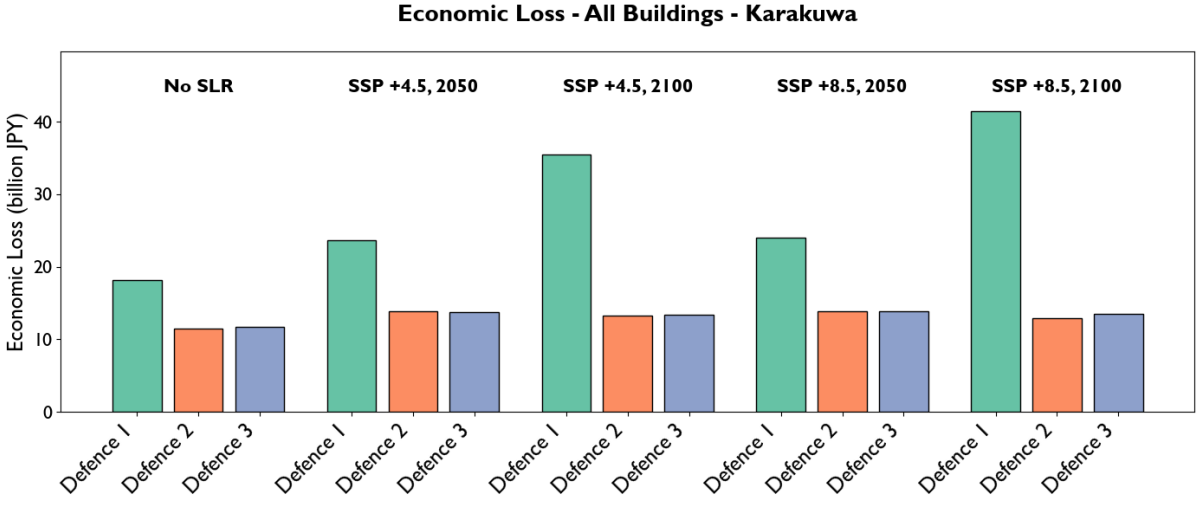

(b)

Fig. 13: Economic loss for all buildings in (a) Kesennuma and (b) Karakuwa. Defence 1 produces consistently higher losses across all scenarios, while Defences 2 and 3 differ only marginally.

https://doi.org/10.5194/egusphere-2026-365
Preprint. Discussion started: 6 February 2026

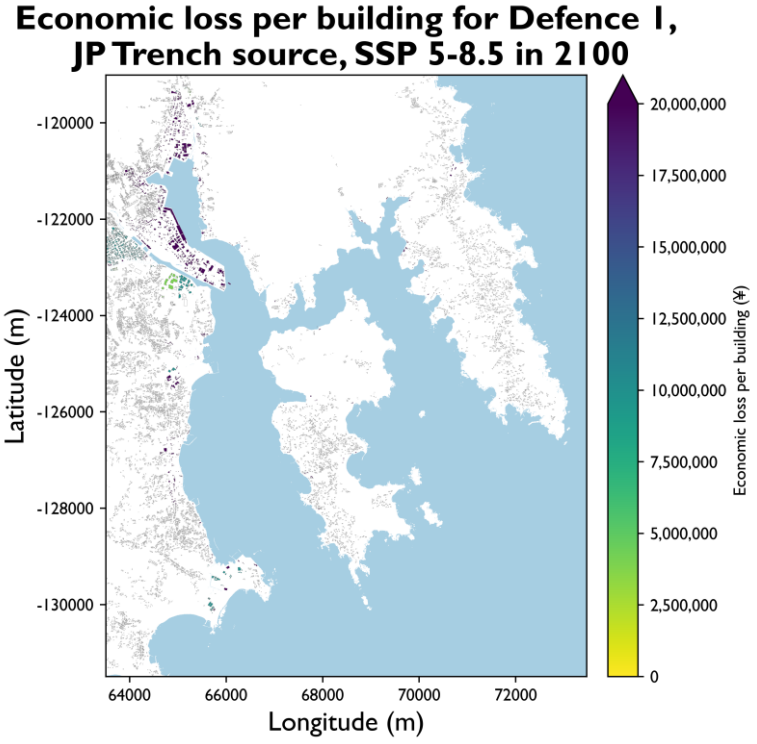

Fig. 14: Spatial distribution of economic loss per building for Defence 1 under the Japan Trench source, SSP5–8.5 scenario in 2100. Loss hotspots are concentrated around Kesennuma's port, waterways, and coastal margins, where inundation depth and building density are highest. Inland and elevated zones exhibit minimal losses due to reduced exposure and topographic protection.

In Karakuwa, overall losses were smaller due to lower population and building density, but the proportional differences between configurations were larger. Defence 3 again achieved the strongest containment, preventing substantial damage to inland settlements. Defence 2 showed similar behaviour with slightly greater exposure along southern bays, while Defence 1 experienced the highest losses, particularly in areas where berms were overtopped.

The consistency of this hierarchy across all emission and SLR conditions confirms that the configuration and continuity of multi-layered systems dominate their capacity to limit financial impacts. Rising sea levels amplify losses across all systems, but the gap between robust and softer defences widens under more extreme conditions, reinforcing the importance of structural integrity for long-term resilience.

https://doi.org/10.5194/egusphere-2026-365
Preprint. Discussion started: 6 February 2026

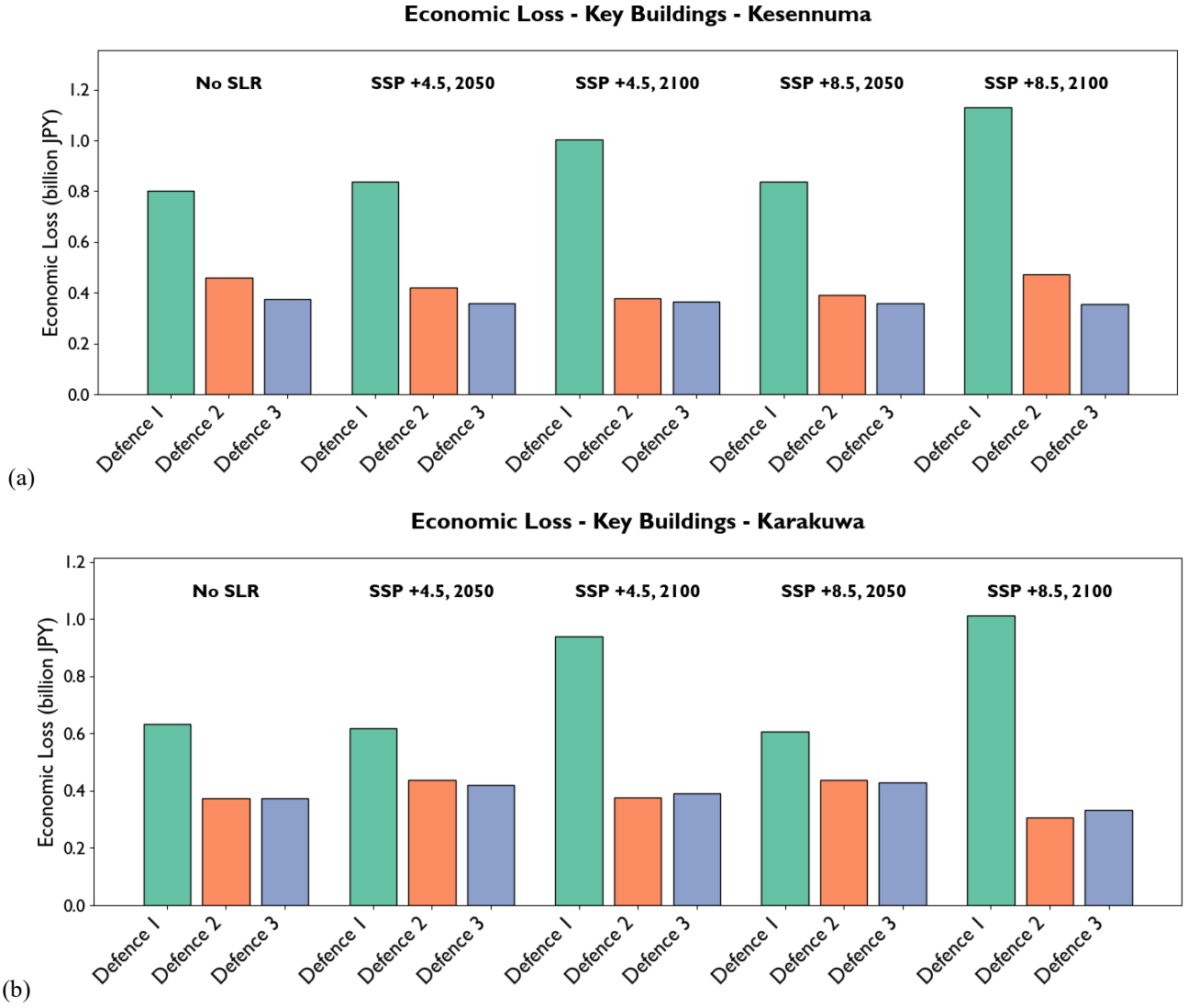

Fig. 15: Economic loss for key buildings in (a) Kesennuma and (b) Karakuwa, mirroring results from all buildings where Defence 1 produces consistently higher losses across all scenarios and Defences 2 and 3 differ only marginally.

5 Discussion

The results demonstrate a clear structural hierarchy across all evaluated indicators, yet the magnitude of difference between the two stronger configurations was smaller than might be expected given their contrasting design philosophies. Defence 2 achieved performance comparable to Defence 3, typically within 10–15 percent across inundation, fatality, and economic loss metrics. Defence 3, which most closely mirrors conventional Japanese coastal engineering, achieved the greatest overall containment but relied heavily on large-scale concrete structures and seawalls that impose significant spatial and visual intrusion. In contrast, Defence 2, designed around transparency, unobstructed visibility, and social openness, achieved nearly

https://doi.org/10.5194/egusphere-2026-365
Preprint. Discussion started: 6 February 2026

equivalent protection with substantially lower physical dominance. This outcome indicates that an open and visually integrated design can maintain technical effectiveness while aligning with HCD priorities. However, it should be noted that the simulated configurations were conceptual rather than physically validated, meaning that their mechanical feasibility, constructability, and long-term maintenance performance were not empirically tested.

The relative performance of Defence 1 further highlights this balance between environmental integration and structural containment. While it embodies Kesennuma's municipal reconstruction principles emphasising ecological harmony and landscape continuity, it consistently exhibited greater inundation spread, slightly higher fatality estimates, and elevated economic losses compared with the other two systems. These outcomes mirror results from other hybrid or nature-based defence studies, which highlight that vegetation and soft materials effectively dissipate flow energy but cannot fully prevent inland propagation during extreme events (Takabatake et al., 2020; Omori et al., 2019). However, in the fatality results, this difference was relatively minor, particularly in Karakuwa, where the elevated terrain and dispersed settlement pattern constrained population exposure. The peninsula's topographic control limited the amplification of fatalities under higher SLR, resulting in only marginal change across all scenarios (Mori et al., 2011; Suppasri et al., 2013; Shibayama et al., 2022). Population data used in the fatality analysis were based on night-time residential distributions derived from national census datasets, meaning that fatalities were only estimated for inhabited areas. As a result, no losses appear within the port, where residential population is absent, even though this area experiences high inundation and economic exposure. This also reflects a limitation of the modelling framework, which parameterised vegetation effects through surface roughness coefficients rather than explicitly modelling stem-scale drag or dynamic deformation, and therefore provides a generalised rather than process-resolved representation of hybrid performance. Defence 1 therefore represents an important complementary layer within a wider system but not a substitute for continuous, engineered protection.

When considering economic loss, the difference between All Building and Key Building impacts reveals further nuances in performance. In both Kesennuma and Karakuwa, the two stronger configurations not only reduced total losses but also provided proportionally greater protection to key buildings, such as schools, hospitals, and civic facilities, whose replacement value and social importance are high. The majority of key buildings are located within Kesennuma's central urban area, near the port and river mouths, where continuous engineered defences play a major role in limiting direct damage. Across all SLR conditions, losses for key buildings increased more gradually than total losses, particularly under Defence 2 and Defence 3, which showed nearly identical performance. This pattern indicates that well-connected, structurally reinforced systems are most effective in safeguarding essential facilities located in the lower-lying urban zones. Comparable results have been reported in previous post-tsunami evaluations, where consistent defence lines around civic clusters reduced infrastructure losses even when residential zones remained partially flooded (Suppasri et al., 2013; Muhari et al., 2018). However, the economic loss model used here assumes uniform building replacement costs and simplified structural typologies, which means variations in construction materials, floor area, or building height were not represented. This simplification limits absolute accuracy but is sufficient to capture relative differences in performance.

https://doi.org/10.5194/egusphere-2026-365
Preprint. Discussion started: 6 February 2026

Across both study sites, the updated fatality results confirm that SLR acts primarily as a background amplifier rather than a determinant of relative performance (Koyano et al., 2022; Church et al., 2013; Suppasri et al., 2013). The ranking of the three systems remains stable under all scenarios, with Defence 2 and Defence 3 maintaining comparable protection and Defence 1 showing only slight performance decline under late-century, high-emission conditions. In Karakuwa, the influence of topography further constrained SLR-driven change, reinforcing that site-specific elevation and exposure characteristics can moderate hazard escalation (Mori et al., 2011; Shibayama et al., 2022). This behaviour aligns with previous observations that small increases in water level can alter tsunami severity through interactions with coastal topography and defence continuity (Mori et al., 2011; Koshimura et al., 2009; Koyano et al., 2022; Church et al., 2013). Nevertheless, SLR increased spatial flood connectivity, especially in low-lying areas of Karakuwa, which led to compounded exposure when flood compartments merged. Because simulations were deterministic, stochastic variability and uncertainty in tsunami generation, source rupture, and local hydrodynamics were not captured. Future applications should employ probabilistic frameworks that incorporate variable source parameters, sediment dynamics, and compound flooding effects.

From a broader perspective, the results align with national and international evidence that continuity and integration of coastal defences, rather than extreme height or rigidity, determine overall system resilience. Koshimura et al. (2009a) and Suppasri et al. (2016) similarly found that once overtopping was prevented along major urban frontages, further reinforcement produced diminishing returns. In this study, Defence 2 achieved near-equivalent outcomes to Defence 3 while incorporating more open and visually integrated design principles, supporting arguments for design optimisation that balances technical performance with aesthetic and social considerations. The practical implication is that defences prioritising openness and spatial integration can maintain effective protection and enhance public acceptance, consistent with post-disaster recovery principles in Japan (Shibayama et al., 2022; Aoki, 2018). Equally, the consistent under-performance of the eco-hybrid Defence 1 reinforces the challenge of translating environmental and social priorities into structural effectiveness. While its vegetated berms and bioswales enhance ecological and visual quality, their lower resistance allows broader shallow flooding, which, although less destructive per building, increases cumulative exposure. This pattern echoes results from hybrid-coast experiments in Japan and Southeast Asia, where partial overtopping and channelisation through vegetation belts limited the protective benefit under large-magnitude forcing (Takabatake et al., 2020; Omori et al., 2019). The results therefore highlight the need to integrate soft measures as secondary buffers within layered systems rather than as stand-alone defences.

Together, these results emphasise that HCD-based tsunami protection does not require a compromise in technical performance. Defence 2 demonstrates that transparent, spatially integrated designs can achieve protection levels comparable to traditional reinforced systems while preserving visual openness and community access, two priorities repeatedly identified in Kesennuma's civic feedback and recovery plans (Leggett et al., 2025; Kesennuma City, 2011). The approach aligns with broader transitions in Japan's DRR policy, which increasingly favours co-existence with water and community-driven design over purely structural isolation (MLIT, 2015). For cities like Kesennuma, where public sentiment remains divided over the

https://doi.org/10.5194/egusphere-2026-365
Preprint. Discussion started: 6 February 2026

sense of safety and spatial separation imposed by high seawalls, the results offer practical evidence that a balanced, participatory design ethos can deliver comparable resilience with greater social legitimacy. Ultimately, while the comparative outcomes are robust, the conceptual and deterministic nature of the modelling framework means results should be interpreted as indicative rather than predictive. More in-depth research should be conducted to extend this framework using probabilistic modelling, empirical testing of materials, and cross-hazard analysis to better capture uncertainty and long-term system evolution.

6 Conclusion

This study evaluated three alternative tsunami defence configurations in Kesennuma using hydrodynamic modelling under multiple SLR scenarios. A consistent performance hierarchy was observed across all metrics: Defence 3 provided the highest containment through large-scale reinforced structures; Defence 2 achieved comparable results, typically within 10–15 percent of Defence 3, while maintaining openness and visual integration; and Defence 1, although aligned with ecological and social goals, offered lower protection but valuable complementary benefits. SLR acted primarily as an amplifier rather than a determinant of performance ranking, highlighting that defence configuration and continuity exert stronger influence than structural height alone. These findings demonstrate that open, HCD based systems can provide robust protection while supporting civic and environmental integration. Future work should incorporate probabilistic modelling and cross-hazard analysis, including storm surges and long-term morphological change. Alternative materials such as glass or hybrid seawalls show potential to enhance transparency and public trust but require empirical validation. Proposed designs should also be presented to residents to assess social acceptability and refine HCD integration. By showing that HCD principles can deliver near-equivalent engineering performance to conventional systems, this study reinforces the need for policy and design approaches that integrate social, environmental, and structural priorities to achieve resilient, community-centred coastal protection.

Data Availability

The bathymetry and topography used in this study were obtained from the high-resolution Sanriku coastal DEM developed by Sugawara, Takahashi and Imamura (2014), originating from the foundational compilation by Takahashi et al. (2000). Model domains, terrain data, and resulting DEMs are available from the corresponding author upon reasonable request due to licensing conditions attached to the original datasets. Tsunami source parameters for the Kuril and Japan Trench scenarios were taken from the Cabinet Office (2020) tsunami hazard assessment and are publicly accessible at: https://www.bousai.go.jp/kouzui/tsunami/chousa/index.html Parameters for the 2011 GEJE source were based on Satake et al. (2013). Sea-level rise projections were obtained using the NASA Sea Level Projection Tool (https://sealevel.nasa.gov/data_tools/17. Land-cover data were sourced from the ESA WorldCover 2020 dataset, available

https://doi.org/10.5194/egusphere-2026-365
Preprint. Discussion started: 6 February 2026

through Google Earth Engine (https://developers.google.com/earth-engine/datasets/catalog/ESA_WorldCover_v100. Building footprint data were obtained from OpenStreetMap (© OpenStreetMap contributors), with extracts generated using BBBike (https://extract.bbbike.org and processed using osmium2shape by Geofabrik (https://geofabrik.de. Population mesh data were derived from official Japanese government statistics (1 km grid), publicly available through the Ministry of Internal Affairs and Communications. The TUNAMI-N2 numerical model used in this study follows the publicly documented framework of Imamura (1996) and Imamura et al. (2006). Model configuration files, custom land-cover reclassification layers, processed OSM building datasets, and all simulation outputs (inundation rasters, flow-depth grids, fatality grids, and economic loss layers) are available from the corresponding author upon reasonable request.

Code Availability

The TUNAMI-N2 model implementation used in this study is based on the publicly documented numerical framework of Imamura (1996) and Imamura et al. (2006). The model source code is distributed by the International Research Institute of Disaster Science (IRIDeS), Tohoku University, and can be obtained upon request from the developers. All pre-processing and post-processing scripts used to generate nested grids, reclassify land-cover data, rasterise building footprints, and compute inundation, fatality, and economic loss metrics were written in Python and MATLAB. These scripts rely on standard open-source libraries (NumPy, SciPy, GDAL, rasterio, geopandas, and MATLAB Mapping Toolbox). Due to containing location-specific input files and IRIDeS-distributed components, the scripts cannot be made fully public but are available from the corresponding author upon reasonable request.

Declaration of competing interest

The authors declare that they have no known competing financial interests or personal relationships that could have appeared to influence the work reported in this paper.

Acknowledgements

This work was supported by JST SPRING - Grant Number JPMJSP2114, the 2024 Tohoku University-University College London Matching Fund and the FY2022 Inter-University Exchange Project Tohoku University.

References

https://doi.org/10.5194/egusphere-2026-365
Preprint. Discussion started: 6 February 2026

References

Aoki, N.: Sequencing and combining participation in urban planning: the case of tsunami-ravaged Onagawa Town, Japan, Cities, 72, 226–236, doi:10.1016/j.cities.2017.08.024, 2018.

Bell, S., MacDonald, D., and Taylor, T.: Establishing a statement of principles for community engagement with civil engineering, Proc. Inst. Civ. Eng. Eng. Sustain., 175, 77–88, 2022.

Bricker, J. D., Gibson, S., Takagi, H., and Imamura, F.: On the need for larger Manning's roughness coefficients in depth-integrated tsunami inundation models, Coast. Eng. J., 57, 1550005, doi:10.1142/S0578563415500056, 2015.

Cabinet Office: Guidelines for post-disaster building damage and economic loss assessment, Government of Japan, Tokyo, 2019.

Cabinet Office, Government of Japan: Japan Trench / Kuril Trench Mega-Earthquake Model Dataset, Cabinet Office, Tokyo, 2020.

Charlesworth, E. and Fien, J.: Design for disaster: community engagement and social sustainability, Archit. Res. Q., 26, 137–148, doi:10.1017/S1359135522000140, 2022.

Chow, V. T.: Open Channel Hydraulics, McGraw-Hill, New York, NY, 1959.

Chua, C. T., Otake, T., Li, T., Cheng, A. C., Qiu, Q., Li, L., Suppasri, A., Imamura, F., and Switzer, A. D.: An approach to assessing tsunami risk to the global port network under rising sea levels, npj Nat. Hazards, 1, 38, doi:10.1038/s44304-024-00039-2, 2024.

Church, J. A., Clark, P. U., Cazenave, A., Gregory, J. M., Jevrejeva, S., Levermann, A., Merrifield, M. A., Milne, G. A., Nerem, R. S., Nunn, P. D., and Payne, A. J.: Sea Level Change, Cambridge University Press, Cambridge, 2013.

Federal Emergency Management Agency (FEMA): Guidelines and specifications for flood hazard mapping partners, FEMA, Washington, DC, 2007.

Federal Emergency Management Agency (FEMA): Hazus–MH Tsunami Model Technical Manual, FEMA, Washington, DC, 2015.

Fuji, K., Suppasri, A., Kwanchai, P., Lahcene, E., and Imamura, F.: Assessing future tsunami hazards from Japan Trench coupling with sea level rise impact on economic risks using an input–output table, Int. J. Disaster Risk Reduct., 104, 104286, doi:10.1016/j.ijdrr.2024.104286, 2024.

Giacomin, J.: What is human centred design?, Des. J., 17, 606–623, doi:10.2752/175630614X14056185480186, 2014.

Goto, C. and Ogawa, Y.: Numerical Method of Tsunami Simulation with the Leap-Frog Scheme, IOC Manual No. 35, UNESCO, Paris, 1997.

Grezio, A., Babeyko, A., Baptista, M. A., Behrens, J., Costa, A., Davies, G., Geist, E. L., Glimsdal, S., González, F. I., Griffin, J., and Harbitz, C. B.: Probabilistic tsunami hazard analysis: multiple sources and global applications, Rev. Geophys., 55, 1158–1198, doi:10.1002/2017RG000579, 2017.

https://doi.org/10.5194/egusphere-2026-365
Preprint. Discussion started: 6 February 2026

Hatamura, Y. and Iino, K.: Lessons learned from the Fukushima accident: management and human factors, J. Nucl. Sci. Technol., 51, 1–16, doi:10.1080/00223131.2013.855164, 2014.

Ishiguro, A. and Yano, E.: Tsunami inundation after the Great East Japan Earthquake and mortality of affected communities, Public Health, 129, 1390–1397, doi:10.1016/j.puhe.2015.08.003, 2015.

Imamura, F.: Review of tsunami simulation with a finite difference method, in: Long-Wave Runup Models, 25–42, 1996.

Imamura, F. and Imteaz, M.: Long waves in two layers: governing equations and numerical model, 1995.

Imamura, F., Yalciner, A. C., and Ozyurt, G.: Tsunami modelling manual, UNESCO IOC Int. Training Course on Tsunami Numerical Modelling, 137–209, 2006.

Kesennuma City: Kesennuma City Earthquake-Reconstruction Plan, Kesennuma City, Kesennuma, 2011.

Koshimura, S., Namegaya, Y., and Yanagisawa, H.: Tsunami fragility: a new measure to identify tsunami damage, J. Disaster Res., 4, 479–488, doi:10.20965/jdr.2009.p0479, 2009a.

Koshimura, S., Oie, T., Yanagisawa, H., and Imamura, F.: Developing fragility functions for tsunami damage estimation using numerical model and satellite imagery, Nat. Hazards, 49, 501–516, doi:10.1007/s11069-008-9302-5, 2009b.

Koshimura, S. and Shuto, N.: Response to the 2011 Great East Japan Earthquake and tsunami disaster, Philos. Trans. R. Soc. A, 373, 20140373, doi:10.1098/rsta.2014.0373, 2015.

Koyano, K., Takabatake, T., Esteban, M., and Shibayama, T.: Magnification of tsunami risks due to sea level rise along the eastern coastline of Japan, J. Coast. Hydraul. Struct., 2, 2022.

Lay, T., Ammon, C. J., Kanamori, H., Koper, K. D., Hutko, A. R., Ye, L., Yue, H., and Rushing, T. M.: The great Sumatra–Andaman earthquake of 26 December 2004, Science, 308, 1127–1133, doi:10.1126/science.1112250, 2005.

Leggett, H., Kitamura, M., Suppasri, A., Imamura, F., and Rossetto, T.: Understanding community attitudes and responses to tsunami mitigation infrastructure and DRR methods in Kesennuma, Japan, Int. J. Disaster Risk Reduct., 105870, doi:10.1016/j.ijdrr.2025.105870, 2025.

Ministry of Land, Infrastructure, Transport and Tourism (MLIT): Technical standards for coastal facilities, MLIT, Tokyo, 2013a.

Ministry of Land, Infrastructure, Transport and Tourism (MLIT): Guidelines for tsunami inundation and damage estimation, MLIT, Tokyo, 2013b.

Ministry of Land, Infrastructure, Transport and Tourism (MLIT): National resilience plan, MLIT, Tokyo, 2015.

Ministry of Land, Infrastructure, Transport and Tourism (MLIT): Flood statistics survey manual, MLIT, Tokyo, 2023.

Mori, N., Takahashi, T., Yasuda, T., and Yanagisawa, H.: Survey of the 2011 Tohoku earthquake tsunami inundation and run-up, Geophys. Res. Lett., 38, L00G14, doi:10.1029/2011GL049210, 2011.

Muhari, A., Imamura, F., Arikawa, T., Hakim, A. R., and Afriyanto, B.: Solving the puzzle of the September 2018 Palu, Indonesia, tsunami mystery, J. Disaster Res., 13, 1058–1070, doi:10.20965/jdr.2018.sc20181108, 2018.

NASA Sea Level Change Team: IPCC AR6 sea level projection tool, NASA Sea Level Portal, 2021.

https://doi.org/10.5194/egusphere-2026-365
Preprint. Discussion started: 6 February 2026

Oetjen, J., Sundar, V., Venkatachalam, S., Reicherter, K., Engel, M., Schüttrumpf, H., and Sannasiraj, S. A.: A comprehensive review on structural tsunami countermeasures, Nat. Hazards, 113, 1419–1449, doi:10.1007/s11069-022-05270-5, 2022.

Okada, Y.: Surface deformation due to shear and tensile faults in a half-space, Bull. Seismol. Soc. Am., 75, 1135–1154, 1985.

Omori, R., Kurosawa, K., and Saito, Y.: Social learning in community-based disaster risk reduction: case studies from Kesennuma, Japan, Int. J. Disaster Risk Reduct., 36, 101100, doi:10.1016/j.ijdrr.2019.101100, 2019.

OpenStreetMap Contributors: Kesennuma building footprint extract, BBBike.org, 2025.

Otsuyama, K. and Shaw, R.: Exploratory case study for neighborhood participation in recovery process, Prog. Disaster Sci., 9, 100141, doi:10.1016/j.pdisas.2021.100141, 2021.

Satake, K.: Geological and historical evidence of irregular recurrent earthquakes and tsunamis at the Japan Trench, Philos. Trans. R. Soc. A, 373, 20140375, doi:10.1098/rsta.2014.0375, 2015.

Satake, K., Fujii, Y., Harada, T., and Namegaya, Y.: Time and space distribution of coseismic slip of the 2011 Tōhoku Earthquake inferred from tsunami waveform data, Bull. Seismol. Soc. Am., 103, 1473–1492, doi:10.1785/0120120122, 2013.

Shibayama, T., Esteban, M., Nistor, I., Takagi, H., Thao, N. D., Matsumaru, R., Mikami, T., Aranguiz, R., Jayaratne, R., and Ohira, K.: Classification of tsunami and evacuation areas, Nat. Hazards, 67, 365–386, doi:10.1007/s11069-013-0570-2, 2013.

Shigihara, Y., Imai, K., Iwase, H., Kawasaki, K., Nemoto, M., Baba, T., Chikasada, N. Y., Chida, Y., and Arikawa, T.: Variation analysis of multiple tsunami inundation models, Coast. Eng. J., 64, 344–371, doi:10.1080/21664250.2021.2010214, 2022.

Shuto, N. and Fujima, K.: A short history of tsunami research and countermeasures in Japan, Proc. Jpn. Acad. Ser. B, 85, 267–275, doi:10.2183/pjab.85.267, 2009.

Strusińska-Correia, A.: Tsunami mitigation in Japan after the 2011 Tōhoku tsunami, Int. J. Disaster Risk Reduct., 22, 397–411, doi:10.1016/j.ijdrr.2017.02.001, 2017.

Sugawara, D. and Goto, K.: Numerical modeling of the 2011 Tohoku-oki tsunami in the offshore and onshore of Sendai Plain, Japan, Sediment. Geol., 282, 110–123, doi:10.1016/j.sedgeo.2012.09.002, 2012.

Sugawara, D., Takahashi, T., and Imamura, F.: Sediment transport due to the 2011 Tohoku-oki tsunami at Sendai, Mar. Geol., 358, 18–37, doi:10.1016/j.margeo.2014.09.002, 2014.

Suppasri, A., Shuto, N., Imamura, F., Koshimura, S., Mas, E., and Yalciner, A. C.: Lessons learned from the 2011 Great East Japan tsunami, Pure Appl. Geophys., 170, 993–1018, doi:10.1007/s00024-012-0511-7, 2013.

https://doi.org/10.5194/egusphere-2026-365
Preprint. Discussion started: 6 February 2026

Suppasri, A., Latcharote, P., Bricker, J. D., Leelawat, N., Hayashi, A., Yamashita, K., Makinoshima, F., Roeber, V., and Imamura, F.: Improvement of tsunami countermeasures based on lessons from the 2011 Great East Japan Earthquake and tsunami, Coast. Eng. J., 58, 1640011, doi:10.1142/S0578563416400118, 2016.

Takabatake, T., Esteban, M., Nistor, I., Shibayama, T., and Nishizaki, S.: Effectiveness of hard and soft tsunami countermeasures on loss of life, Int. J. Disaster Risk Reduct., 45, 101491, doi:10.1016/j.ijdrr.2019.101491, 2020.

Tanikawa, H., Sugimoto, K., Okuoka, K., and Akiyama, Y.: Estimation of lost building stock due to the 2016 Kumamoto earthquakes, J. Jpn. Soc. Civ. Eng. Ser. G, 73, II_293–II_300, doi:10.2208/jscejer.73.II_293, 2017.

Tashiro, A. and Sakisaka, K.: Model analysis of residents' consciousness regarding seawall construction, Chiikigaku Kenkyu, 45, 419–433, 2015.

Ueda, Y. and Shaw, R.: Community recovery in tsunami-affected area: lessons from Minami-Kesennuma, in: Tohoku Recovery, Springer Japan, Tokyo, 131–146, 2014.

United Nations Office for Disaster Risk Reduction: Global Assessment Report on Disaster Risk Reduction 2022, UNDRR, Geneva, 2022.

USACE: Hydrologic Engineering Center – River Analysis System (HEC-RAS) User's Manual, Version 5.0.7, U.S. Army Corps of Engineers, Davis, CA, 2020.

Welsh, R., Williams, S., Bosserelle, C., Paulik, R., Chan Ting, J., Wild, A., and Talia, L.: Sea-level rise effects on changing hazard exposure to far-field tsunamis, J. Mar. Sci. Eng., 11, 945, doi:10.3390/jmse11050945, 2023.

Wolff, E.: The promise of a people-centred approach to floods, Prog. Disaster Sci., 10, 100171, doi:10.1016/j.pdisas.2021.100171, 2021.

Yanagisawa, H., Koshimura, S., Goto, K., Miyagi, T., Imamura, F., Ruangrassamee, A., and Tanavud, C.: Reduction effects of mangrove forest on a tsunami, Estuar. Coast. Shelf Sci., 81, 27–37, doi:10.1016/j.ecss.2008.10.020, 2009.

Yeh, H., Liu, P., and Synolakis, C.: Tsunami research since 2004: achievements and future challenges, Pure Appl. Geophys., 170, 1115–1128, doi:10.1007/s00024-011-0423-1, 2012.

Zanaga, D., Van De Kerchove, R., De Keersmaecker, W., Souverijns, N., Brockmann, C., Quast, R., Wevers, J., Grosu, A., Paccini, A., Vergnaud, S., Cartus, O., Santoro, M., Fritz, S., Georgieva, I., Lesiv, M., Carter, S., Herold, M., Li, L., Tsendbazar, N. E., Ramoino, F., and Arino, O.: ESA WorldCover 10 m 2020 v100, Zenodo, doi:10.5281/zenodo.5571936, 2021.